

Chapter 5.

FIELD QUALITY IMPROVEMENTS AFTER CONSTRUCTION

The research work described in this chapter is partly based on the following papers :

- R.C. Gupta, *Correcting Field Harmonics after Design in Superconducting Magnets*, Proceedings of the 4th International Industrial Symposium on Super Collider (IISSC), New Orleans, pp. 773-780 (1992).
- R. Gupta, *Iron Shims to Correct the Measured Harmonics in 130 mm Aperture RHIC Insertion Quadrupoles*, Magnet Division Internal Note 480-16 (RHIC-MD-185), Dec. 10, 1992, Unpublished (1992).
- R. Gupta, et al., *Large Aperture Quadrupoles for RHIC Interaction Regions*, Proceedings of the 1993 Particle Accelerator Conference, Washington, D.C., pp. 2745-2747 (1993).
- R. Gupta, et al., *Field Quality Improvements in Superconducting Magnets for RHIC*, Proceedings of the 1994 European Particle Accelerator Conference, London, UK, pp. 2928-2930 (1994).
- R. Gupta, et al., *Tuning Shims for High Field Quality in Superconducting Magnets*, Proceedings of the Fourteenth International Conference on Magnet Technology (MT-14), Tampere, Finland, June 11-16 (1995).
- R. Gupta, *Field Quality in the Superconducting Magnets for Large Particle Accelerators*, Proceedings of the 1996 European Particle Accelerator Conference at Sitges, Spain (1996).

5.1. Introduction

The field quality in superconducting magnets is mainly determined by the following three factors :

- (a) The inherent harmonic components in the magnetic design
- (b) The errors in the dimensions of the parts used in making the magnets
- (c) The errors (non-reproducible distortions) in the magnets

(a) was discussed in chapters 2 and 3 where the field quality improvements through yoke and coil designs were discussed. In this chapter methods to overcome the limitations posed by (b) and (c), which usually determine the ultimate field quality in superconducting magnets, are developed. The tolerances in components, in manufacturing and in the assembly are typically of the order of $25\text{-}50\mu\text{m}$. An attempt to improve on those mechanical tolerances would be too expensive and too demanding, so for all practical purposes the field errors from them set the limit on the expected field quality in superconducting magnets. However, sometimes the performance of a machine may be limited by these harmonics.

To overcome these limitations, methods are developed here which correct or compensate for the measured harmonics after the construction of a magnet is partly complete. These corrections are applied either at the body of the magnet or lumped at the ends of the magnet. First, the “tuning shim” method is discussed, which is applied in the body of the magnet. Then in the next section, the “ a_1 correction” method is discussed which is applied at the ends of the magnet. Neither of the two methods requires disassembling the already built magnet. The relative field errors ($\Delta B/B$) in superconducting magnets are generally of the order of 10^{-4} at $2/3$ of the coil radius. These methods can reduce these relative field errors by about an order of magnitude provided that the harmonic measurements are reliable and the harmonic contents in the magnets are reproducible after quench and thermal cycles.

A correction in the field non-uniformity by attaching iron shims on the yoke surface is now routinely made in MRI (Magnetic Resonance Imaging) magnets and has also been used in window frame [39] magnets. The use of iron shim methods in superconducting accelerator magnets based on methods similar to those discussed here has been proposed elsewhere [50,81].

5.2. Tuning Shims in Magnet Body for Extra High Field Quality

A tuning shim correction method has been incorporated in the basic design of the 130 mm aperture RHIC insertion quadrupoles to compensate the measured field harmonics in the body of the magnet. The length of these tuning shims is the same as the mechanical length of the magnet. They are made partly of magnetic and partly of non-magnetic material with the actual composition of each shim determined by the harmonics in an individual magnet. The tuning shim method described here can reduce the targeted harmonics to a level where the value of them is determined only by the measurement and reproducibility errors in the magnets.

The subsequent discussion here is limited to the RHIC insertion quadrupoles, but the basic principle and method could apply to any superconducting magnet design. In the following sub-sections the principle of the tuning shim correction, the basic magnet and tuning shim design, the procedure for implementing it in the magnet, the calculations, and a comparison between the calculations and the measurements will be discussed.

5.2.1. Tuning Shims in the RHIC Interaction Region Quadrupoles

To obtain a high luminosity (a term used in specifying the probability of interaction of particle beams in collision) for a given number of particles in the beam, the beam is squeezed to a very small size at the crossing (collision) point. This is called the low β^* squeeze as the $\sqrt{\beta}$ is proportional to beam size. An unavoidable consequence is an increase in beam size in the quadrupoles located on either side of the crossing point. The maximum tolerable beam size is determined by the field quality in the magnets since the physical aperture is more than the good field aperture. In RHIC the ultimate luminosity performance is determined by the field quality in the interaction region quadrupoles used in the “low β^* ” focussing triplet. To overcome the usual mechanical limitations on field quality a method of *Tuning Shims* has been developed for the 130 mm aperture RHIC interaction region quadrupoles. The method is referred to as the *Tuning Shim Method* because it corrects the measured harmonics in an individual magnet by adjusting (tuning) the amount of iron in each of several tuning shims. Such methods have been previously used to obtain a high field uniformity in room temperature, window-frame, iron-dominated magnets.

The basic principle behind this passive correction method is to place magnetic material (shims) at the inside surface of the yoke aperture. There, it is magnetized and creates

a large local distortion in the magnetic field as well as a significant change in the shape of the field at the center of the magnet. This change in field shape can be expressed in terms of harmonic components. By properly choosing the locations and dimensions of these magnetic shims one can cancel out the field errors. The number of measured harmonics which can be independently optimized using this method is equal to or less than the number of shims used. An undesired effect of this method is that in the process of correcting lower order harmonics, higher order harmonics are also generated. However, the location of the shims can be chosen to minimize these higher order effects. The location of these shims is also chosen to minimize iron saturation effects. This requires that the tuning shims be put as close to the yoke aperture as possible.

In the 130 mm aperture RHIC interaction region quadrupoles, eight tuning shims are used. They are used to correct eight harmonics — a_2 through a_5 and b_2 through b_5 . Physically a single tuning shim is a package of epoxied laminations. The thickness of the package is constant, but some of the laminations are made of magnetic low carbon steel and some are made of non-magnetic brass. The adjustment (tuning) of the harmonics is achieved by varying the ratio of magnetic to non-magnetic laminations in the eight shims.

5.2.2. Tuning Shim and the Magnet Design

The magnetic lengths of the three interaction region quadrupoles in the focusing triplet are 1.44 m, 3.4 m and 2.1 m. They all have the same cross section. The cross section of these magnets is shown in Fig. 5.2.1 which also shows the locations of the eight tuning shims 1A through 4B. The complete design of this magnet will be described in detail in chapter 6. The yoke inner surface consists of two circular radii instead of the usual one radius to reduce the saturation induced b_5 . The yoke inner radius is 87 mm at the midplane and 92 mm at the pole. The space between the coil and yoke is filled with a thin, glass-filled, phenolic spacer. The outer surface of the spacer also has two radii, 87 mm at the midplane and 92 mm at the pole. However, eight gaps are left between the yoke and phenolic spacer. The location of gap 2B in the first octant is about 30° . The location of the other seven gaps is determined by the quadrupole symmetry, for example gap 2A is at 60° , 1B is at 120° , etc. (see Fig. 5.2.1).

A schematic diagram of the tuning shim in the magnet at location 1B is also shown in Fig. 5.2.1. The actual tuning shim is a package of a number of low carbon steel (magnetic) and brass (non-magnetic) laminations. The use of laminations assures small eddy currents. These laminations have a width of 6.6 mm and a thickness of either 0.13 mm or 0.51 mm. The total thickness of all laminations in each tuning shim package is always 6.1 mm, but the proportion of iron laminations varies. The lamination pack is cured into a parallelogram shape in a fixture with epoxy between the laminations. At the end of the curing cycle the tuning shim package is quite sturdy and can be handled easily. The width of the lamination pack is 7.5 mm and the thickness is 6.35 mm (6.1 mm laminations and 0.25 mm epoxy). These dimensions provide a small but sufficient clearance for easy insertion of the tuning shims into the magnet. The two thicknesses of laminations (0.13 mm and 0.51 mm) provide the necessary resolution in the harmonic correction while keeping the number of laminations to a reasonable value. The nominal magnetic thickness of the tuning shim is 3.175 mm, of which 3.05 mm is occupied by the iron laminations; the presence of the epoxy reduces the iron packing factor by $\sim 4\%$. A composition of the tuning shim package is shown in Fig. 5.2.2 where one side of the tuning shim is shown in more detail. The steel shims are actually the iron laminations which define the magnetic thickness of the tuning shim.

The tuning shims are placed such that the iron laminations are next to the yoke to provide a better magnetic circuit. This has been done to minimize the difference in harmonic

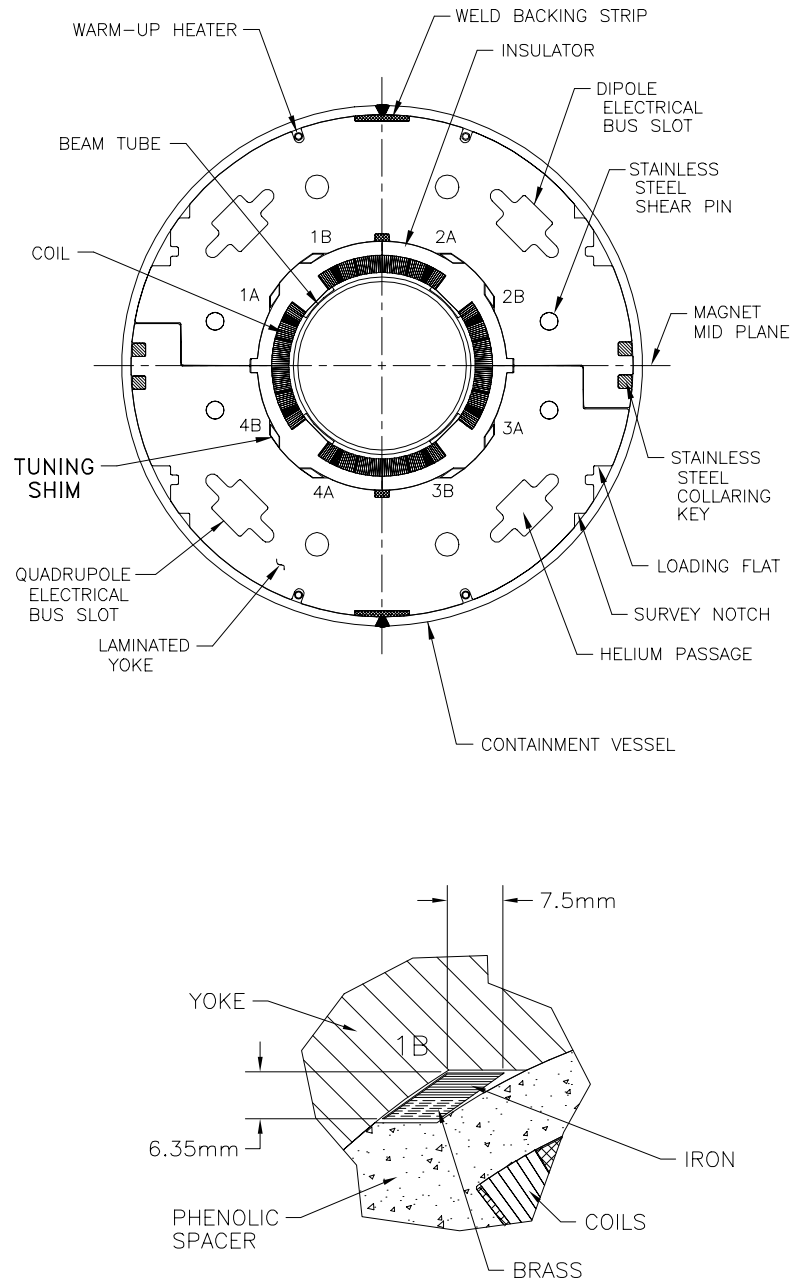


Figure 5.2.1: The upper drawing shows the cross section of the 130 mm aperture RHIC interaction quadrupoles. 1A, 1B, etc. are the locations of eight gaps for tuning shims. The lower drawing shows the tuning shim placed at location 1B in the magnet. There are eight such shims in every magnet, each having the same total size but a variable composition of brass and low carbon steel.

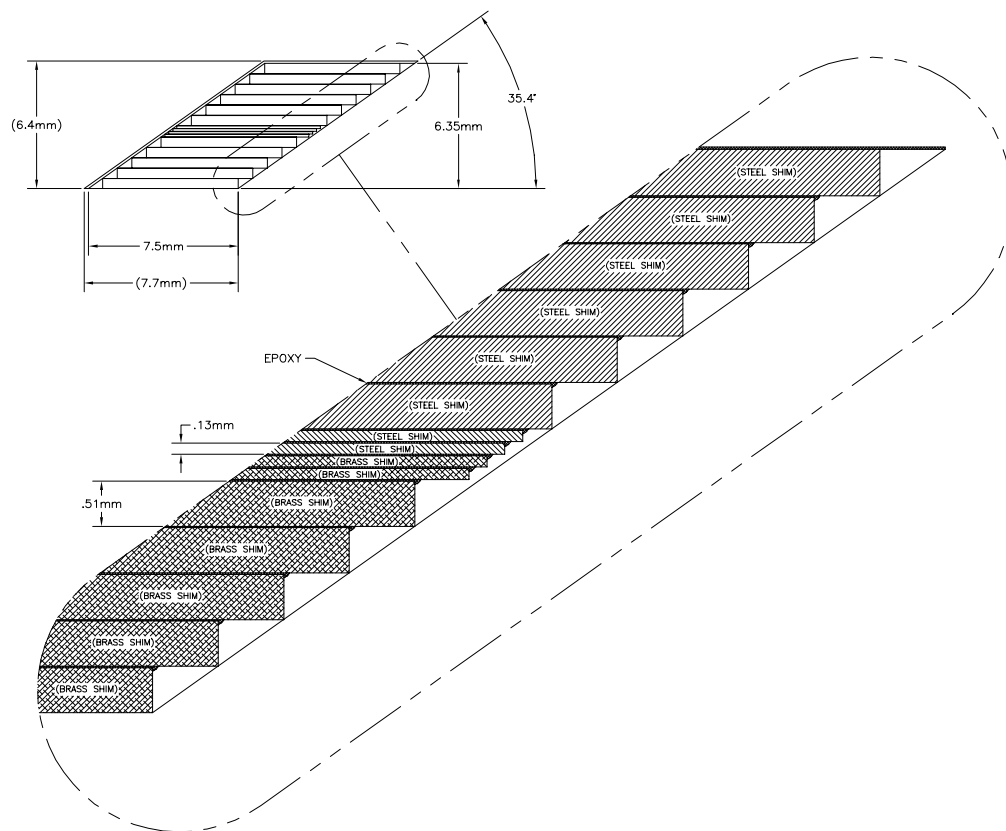


Figure 5.2.2: A composition of the tuning shim package where one side of the tuning shim is shown in more detail. The steel shims are actually the iron laminations which defines the magnetic thickness of the tuning shim. There are 11 laminations (brass or steel) having a thickness of 0.51 mm and four of .13 mm. The epoxy provides a bond between them after curing.

compensation between low current and high current due to iron saturation. However, a small gap is left for the following reasons :

- (a) a mismatch in yoke and tuning shim geometries (the yoke inner surface is circular and the defining surface of the shim package is flat)
- (b) the actual shape of the tuning shim package is a staircase in which each rectangular lamination is displaced by a small amount to create a parallelogram shape.
- (c) a 0.1 mm thick Kapton sheet is used between the tuning shim and the yoke to provide insulation against eddy currents between the two.
- (d) a small clearance is needed for easy insertion of the tuning shims in the magnet. Once the quadrupole is energized, the magnetic attraction between the yoke-iron and lamination-iron pulls the tuning shims close to the yoke inner surface.

5.2.3. Procedure for Implementing the Tuning Shim Correction

The complete procedure for installing tuning shims to compensate the field harmonics involves the following steps:

1. Measure the harmonics in the absence of tuning shims,
2. Compute the thickness of magnetic material in each of the eight tuning shims needed to obtain the desired change in eight harmonics,
3. Make eight tuning shims. Each tuning shim is a package that consists of a number of magnetic steel and non-magnetic brass laminations cured to a fixed dimension,
4. Install the eight tuning shims in the magnet at the proper locations, and
5. Measure the field harmonics with the tuning shims installed, for verification.

Since the highest luminosity is desired at the top energy, ideally the magnetic measurements in step 1 should be performed at the maximum operating current which is about 5 kA. However, this would require a costly cryogenic test. To save on the time and cost of the initial magnetic measurements, the field harmonics are measured first at room temperature. It is known by the measurements that, except for a systematic shift (change) in the harmonics allowed by the magnetic geometry, the values of the warm and cold harmonics

are nearly the same. Therefore, to a reasonable certainty, one is able to predict the values of field harmonics at 5 kA from the warm measurements of the field harmonics.

The thickness of the magnetic material in the tuning shims in step 2 above is therefore, computed based on the warm measurements. The thickness of iron laminations in the eight tuning shim is computed such that they compensate for the harmonics in the straight section (body) of the magnet. As mentioned earlier, the eight tuning shims would have different proportions of iron in them to correct the eight harmonics a_2 through a_5 and b_2 through b_5 . A computer code *SHIMCAL* [68] has been developed which computes the number of magnetic laminations needed in each of the eight tuning shim locations to produce the required change in the eight harmonics. Ideally these harmonics (except for b_5) should be zero at 5 kA after the tuning shims are installed. The design value of b_5 in the straight section is -1.2 unit [171] to compensate for a large b_5 in the magnet ends. In reality, however, a small component may be left because of the limited resolution in the thickness of laminations and because of various other errors involved in the process and in harmonic measurements. However, these residual harmonics are expected to be about an order of magnitude smaller than has been achieved in previous superconducting magnets.

The procedure for manufacturing the tuning shims (step 3) has been described in the previous section.

The eight tuning shims are inserted (step 4) from the return end (non-lead end) of the magnet in the eight pre-defined spaces in the magnet as shown in Fig. 5.2.1. The tuning shims are inserted such that the magnetic laminations are closest to the yoke inner surface. The magnets are not disassembled to install the tuning shims. It may be pointed out that if the magnet is disassembled and reassembled, the field harmonics may change in the process. This is due to small differences in the mechanics involved in the collaring process, which can not be reproduced. Because of these differences, the conductors in the re-collared coil do not go exactly to the same original location. Although these differences may only be of the order of 25 μm , they produce harmonic changes that are larger than desired in these highly accurate magnets. Therefore, the design feature that allows the shim to be installed without opening the magnet not only makes the process more efficient but also removes the harmonics that would have been created in the reassembly process.

The harmonics are re-measured after the shims are installed (step 5). First they are measured warm for a quick check that (a) the magnetic laminations in the eight tuning shims have the correct thickness, and (b), all of the eight shims have been installed at the

correct locations and in the correct orientation. If the warm measurements show any error, the shims can be easily taken out and installed again in a relatively short period of time as compared to the time required for a cold test. The warm measurements should show an over-compensation in field harmonics. This is necessary because a part of the compensation is lost at 5 kA due to the saturation of the iron in the tuning shims. Finally, the actual values of field harmonics after shim correction are measured at 5 kA after the magnet is cooled to ~ 4.5 K.

5.2.4. Calculations for Tuning Shim Corrections

In this section calculations for the field harmonics produced by magnetic tuning shims of various thickness are presented. In the nominal design, with the nominal size tuning shims, the change over from iron to brass occurs at about 30° , in the first octant, as shown in Fig. 5.2.1. The eight diamond-shaped tuning shims are placed in these eight locations in such a way that the two iron surfaces of the tuning shim are as close to the two yoke inner surface as possible. However, as mentioned earlier, a small gap between the two surfaces is left for various assembly reasons. Inclusion of such gaps in computer models produces a mesh that may create large errors in the numerical calculations. Moreover, no method is known to include these gaps in analytic calculations that would account for saturable iron in such a geometry. However, to help understand the magnitude of harmonics by tuning shims and to understand geometric and symmetry effects, approximate analytic expressions are obtained even though they do not quite represent the actual problem.

Analytic expressions for the field harmonics produced by the magnetic tuning shims are difficult to obtain due to the following reasons : (a) the shims have a large size and complex shape, (b) the permeability of the iron (both in the tuning shim region and in the yoke iron) is not constant and varies by a large amount and (c) the shims are located where the yoke aperture is not defined by a simple circular geometry (for which the analytic expressions are easier to derive) but instead is described by two radii in a complex geometry. Therefore analytic methods are used only to help understand symmetry etc., and numerical methods are used for quantitative calculations. The computer code used for the numerical work is POISSON; however the calculations have been verified with results obtained with the codes PE2D and MDP.

5.2.4.1. Approximate Analytic Expressions for Low Field Estimate

Approximate analytic expressions for the harmonics generated by an iron shim at the yoke inner surface can be derived using the first order perturbation theory such as that used by Halbach [81]. In order to obtain expressions the following assumptions and modifications are made for simplification : (a) The yoke inner surface is described by a circular geometry (rather than two radii) having a constant radius R_f throughout the aperture, (b) the field at the yoke inner surface is low and the permeability (μ) of the iron is constant (c) the field at (inside) the yoke inner surface is perpendicular to it (d) the perturbation is small, and the shim has a radial thickness Δt small compared to the radius R_f and an angular width $\Delta\theta$ (between angles θ_0 and $\theta_0 + \Delta\theta$) small compared $\frac{\pi}{m}$. Though none of these assumptions are valid in the geometry (2-radius aperture) and field (high field where iron is saturated) under consideration, nevertheless, the analytic expressions are obtained to develop a conceptual understanding. For example these expressions would correctly predict the symmetry between the harmonics generated by tuning shims in various locations. Since the agreement is not good, no attempt will be made to compare the measurements with the analytic expressions; the measurements will be compared with the numerical calculations.

Following a procedure similar to that discussed by Halbach [81] the effect of a tuning shim to first order is described by changing the radial component of the field at the iron surface. This perturbation and the inverse Fourier transformations given in Eq. (1.5.33c) and Eq. (1.5.33h) are used to compute the change in the field harmonics (convention : b_2 for normal sextupole) due to this additional iron in the tuning shim as follows :

$$\Delta a_n = \frac{10^4}{\pi B_{R_0}} \int_{R_f - \Delta t}^{R_f} \left(\frac{R_0}{r} \right)^n \frac{dr}{r} \int_{\theta_0}^{\theta_0 + \Delta\theta} \Delta B_r(r, \theta) \cos((n+1)\theta) d\theta, \quad (5.2.1a)$$

$$\Delta b_n = \frac{10^4}{\pi B_{R_0}} \int_{R_f - \Delta t}^{R_f} \left(\frac{R_0}{r} \right)^n \frac{dr}{r} \int_{\theta_0}^{\theta_0 + \Delta\theta} \Delta B_r(r, \theta) \sin((n+1)\theta) d\theta, \quad (5.2.1b)$$

where B_{R_0} is the unperturbed field on the median plane at $x = R_0$ and $\Delta B_r(r, \theta)$ is the incremental radial component of the field due to the shim iron. The incremental field is computed at the yoke inner surface where the tuning shims are placed. The radial component of the field inside the yoke inner surface (air region) in the case of an ideal $2m$ -pole magnet with a current sheet at a radius a having a distribution $I(a, \theta) = I_0 \cos(m\theta)$ is given in chapter 1 (see Eq. (1.5.115a)). The shim iron enhances this field by μ and therefore,

the incremental field due to the shim iron is given by :

$$\Delta B_r(r, \theta) = -\frac{\mu_o I_o}{2a} \left(1 + \frac{\mu - 1}{\mu + 1} \left(\frac{r}{R_f} \right)^{2m} \frac{\left[1 - \left(\frac{R_f}{R_a} \right)^{2m} \right]}{\left[1 - \left(\frac{\mu - 1}{\mu + 1} \right)^2 \left(\frac{R_f}{R_a} \right)^{2m} \right]} \right) \times (\mu - 1) \left(\frac{a}{r} \right)^{m+1} \sin(m\theta). \quad (5.2.2)$$

Let

$$F_\mu = \frac{\mu - 1}{\mu + 1} \frac{\left[1 - \left(\frac{R_f}{R_a} \right)^{2m} \right]}{\left[1 - \left(\frac{\mu - 1}{\mu + 1} \right)^2 \left(\frac{R_f}{R_a} \right)^{2m} \right]}, \quad (5.2.3)$$

which is just $\frac{\mu - 1}{\mu + 1}$ for $R_a \gg R_f$. Using F_μ in Eq. (5.2.2) one gets :

$$\Delta B_r(r, \theta) = -\frac{\mu_o I_o}{2a} (\mu - 1) \left(1 + F_\mu \left(\frac{r}{R_f} \right)^{2m} \right) \sin(m\theta) \left(\frac{a}{r} \right)^{m+1}. \quad (5.2.4)$$

B_{R_0} , the field at $x = R_0$ is obtained from Eq. (1.5.112) as

$$B_{R_0} = -\frac{\mu_o I_o}{2a} \left(1 + F_\mu \left(\frac{a}{R_f} \right)^{2m} \right) \left(\frac{R_0}{a} \right)^{m-1}, \quad (5.2.5)$$

where F_μ is defined in Eq. (5.2.3).

Substituting Eq. (5.2.2) and Eq. (5.2.5) in Eqs. (5.2.1) and simplifying, one obtains :

$$\Delta a_n = K_n \int_{\theta_0}^{\theta_0 + \Delta\theta} \sin(m\theta) \cos((n+1)\theta) d\theta, \quad (5.2.6a)$$

$$\Delta b_n = K_n \int_{\theta_0}^{\theta_0 + \Delta\theta} \sin(m\theta) \sin((n+1)\theta) d\theta, \quad (5.2.6b)$$

with

$$K_n = \frac{(\mu - 1) 10^4 R_0^{n-m+1} a^{2m}}{\pi \left(1 + F_\mu \left(\frac{a}{R_f} \right)^{2m} \right)} \int_{R_f - \Delta t}^{R_f} \left(\frac{1}{r^{n+m+1}} + \frac{F_\mu}{R_f^{2m}} r^{m-n-1} \right) dr. \quad (5.2.7)$$

On integration one obtains :

$$K_n = -\frac{(\mu - 1) 10^4 R_0^{n-m+1} a^{2m}}{\pi \left(1 + F_\mu \left(\frac{a}{R_f} \right)^{2m} R_f^{n+m} \right)} \times \left[\frac{1 - \left(1 - \frac{\Delta t}{R_f} \right)^{-(n+m)}}{n+m} - F_\mu \frac{1 - \left(1 - \frac{\Delta t}{R_f} \right)^{(n-m)}}{n-m} \right]. \quad (5.2.8)$$

For $\Delta t \ll R_f$, this becomes :

$$K_n = \frac{(\mu - 1) 10^4 R_0^{n-m+1} a^{2m}}{\pi \left(1 + F_\mu \left(\frac{a}{R_f} \right)^{2m} R_f^{n+m} \right)} \times \frac{(1 - F_\mu) \Delta t}{R_f}. \quad (5.2.9)$$

To solve Eqs. (5.2.6) completely, the integration is performed over the angle to obtain :

$$\begin{aligned} \Delta a_n = K_n & \left(\frac{\cos [(n+1+m)(\theta_0 + \Delta\theta)] - \cos [(n+1+m)\theta_0]}{n+1+m} \right) \\ & - K_n \left(\frac{\cos [(n+1-m)(\theta_0 + \Delta\theta)] - \cos [(n+1-m)\theta_0]}{n+1-m} \right) \end{aligned} \quad (5.2.10a)$$

$$\begin{aligned} \Delta b_n = K_n & \left(\frac{\sin [(n+1+m)(\theta_0 + \Delta\theta)] - \sin [(n+1+m)\theta_0]}{n+1+m} \right) \\ & - K_n \left(\frac{\sin [(n+1-m)(\theta_0 + \Delta\theta)] - \sin [(n+1-m)\theta_0]}{n+1-m} \right) \end{aligned} \quad (5.2.10b)$$

For small $\Delta\theta$ the Eqs. (5.2.6) reduces to :

$$\Delta a_n = K_n \cos((n+1)\theta_0) \sin(m\theta_0) \Delta\theta \quad (5.2.11a)$$

$$\Delta b_n = K_n \sin((n+1)\theta_0) \sin(m\theta_0) \Delta\theta \quad (5.2.11b)$$

As a reminder $n=0$ is dipole and the current distribution for creating a dipole field is $m=1$.

5.2.4.2. Numerical Calculations for Low Field Correction

In this section, the results of calculations are given for the field harmonics produced by magnetic shims in the low current (field) case. At low field, the permeability of the iron is large and to a sufficient accuracy, the iron can be considered to have a field-perpendicular boundary condition. In this case, the harmonics do not show any current dependence. The small gap between the tuning shim and the yoke aperture is ignored. The shim thickness is changed in steps of 0.020" (0.51 mm). The change for a shim of given thickness is computed going from the no-shim case (rather than the nominal shim case).

The computed harmonics are listed in selected cases. In Table 5.2.1 they are given for a shim thickness of 0.060" (1.52 mm), in Table 5.2.2 for 0.120" (3.05 mm), in Table 5.2.3 for 0.180" (4.57 mm) and in Table 5.2.4 for a shim thickness of 0.240" (6.10 mm) respectively. The above changes are computed going from the no-shim case. The capability of tuning shims to correct the measured harmonics is computed from the nominal case for which the average thickness of the tuning shims is 0.120" (3.05 mm), half of the maximum value. In this shifted system, the thickness of the tuning shims is negative if the magnetic part of the shim is smaller than nominal.

Table 5.2.1: Computed low field change in harmonics caused by 1.52 mm (0.060") thick magnetic tuning shims at the given location, LOC, (see Fig. 5.2.1). The transfer function is given in T/m/kA.

LOC	δTF	δa_0	δa_1	δa_2	δa_3	δa_4	δa_5	δa_6	δa_7	δa_8	δa_9
None	0.000	0.00	0.00	0.00	0.00	0.00	0.00	0.00	0.00	0.00	0.00
1A	0.0033	3.61	-1.60	-0.38	1.03	-0.83	0.45	-0.17	0.03	0.02	-0.022
1B	0.0033	2.32	1.60	-2.58	1.03	0.26	-0.45	0.17	0.03	-0.06	0.023
2A	0.0033	2.32	-1.60	-2.59	-1.03	0.26	0.45	0.17	-0.03	-0.06	-0.022
2B	0.0033	3.60	1.59	-0.38	-1.03	-0.83	-0.45	-0.17	-0.03	0.02	0.024
3A	0.0033	-3.60	-1.60	0.38	1.03	0.83	0.45	0.17	0.025	-0.03	-0.02
3B	0.0033	-2.32	1.60	2.58	1.033	-0.26	-0.45	-0.17	0.03	0.058	0.02
4A	0.0033	-2.32	-1.60	2.58	-1.03	-0.26	0.45	-0.17	-0.03	0.057	-0.02
4B	0.0033	-3.61	1.60	0.38	-1.03	0.83	-0.45	0.17	-0.03	-0.018	0.02
ALL	0.0267	0.00	0.00	0.00	0.00	0.00	0.00	0.00	0.00	0.00	0.00
LOC	TF	δb_0	b_1	δb_2	δb_3	δb_4	δb_5	δb_6	δb_7	δb_8	δb_9
None	9.4889	0.00	10 ⁴	0.00	0.00	0.00	0.00	0.00	0.00	0.00	0.00
1A	9.4923	-2.32	10 ⁴	-2.59	1.18	-0.26	-0.12	0.17	-0.12	0.06	-0.02
1B	9.4923	-3.59	10 ⁴	-0.38	-1.18	0.83	-0.12	-0.17	0.12	-0.02	-0.02
2A	9.4923	3.60	10 ⁴	0.38	-1.18	-0.83	-0.12	0.17	0.12	0.02	-0.02
2B	9.4923	2.32	10 ⁴	2.58	1.18	0.26	-0.12	-0.17	-0.12	-0.06	-0.02
3A	9.4923	2.32	10 ⁴	2.58	1.18	0.26	-0.12	-0.17	-0.12	-0.06	-0.02
3B	9.4923	3.60	10 ⁴	0.38	-1.18	-0.83	-0.12	0.17	0.12	0.02	-0.02
4A	9.4923	-3.60	10 ⁴	-0.38	-1.18	0.83	-0.12	-0.17	0.12	-0.02	-0.02
4B	9.4923	-2.32	10 ⁴	-2.58	1.18	-0.26	-0.12	0.17	-0.12	0.06	-0.02
ALL	9.5156	0.00	10 ⁴	0.00	0.00	0.00	-0.93	0.00	0.00	0.00	-0.16

Table 5.2.2: Computed low field change in harmonics caused by 3.05 (0.120") thick magnetic tuning shims at the given location, LOC, (see Fig. 5.2.1). The transfer function is given in T/m/kA.

LOC	δTF	δa_0	δa_1	δa_2	δa_3	δa_4	δa_5	δa_6	δa_7	δa_8	δa_9
None	0.000	0.00	0.00	0.00	0.00	0.00	0.00	0.00	0.00	0.00	0.00
1A	0.0075	7.87	-3.31	-1.08	2.43	-1.87	0.96	-0.33	0.03	0.06	-0.055
1B	0.0075	5.23	3.31	-5.67	2.43	0.44	-0.96	0.41	0.03	-0.12	0.055
2A	0.0075	5.23	-3.31	-5.67	-2.43	0.44	0.96	0.41	-0.03	-0.12	-0.0055
2B	0.0074	7.85	3.30	-1.08	-2.43	-1.87	-0.96	-0.33	-0.03	0.06	0.055
3A	0.0075	-7.87	-3.31	1.08	2.43	1.87	0.96	0.33	0.03	-0.06	-0.055
3B	0.0075	-5.23	3.31	5.67	2.43	-0.44	-0.96	-0.41	0.03	0.12	0.055
4A	0.0074	-5.22	-3.30	5.67	-2.43	-0.44	0.96	-0.41	-0.03	0.12	-0.055
4B	0.0075	-7.87	3.30	1.08	-2.43	1.87	-0.96	0.33	-0.03	-0.06	0.055
ALL	0.0595	0.00	0.00	0.00	0.00	0.00	0.00	0.00	0.00	0.00	0.00
LOC	TF	δb_0	b_1	δb_2	δb_3	δb_4	δb_5	δb_6	δb_7	δb_8	δb_9
None	9.4889	0.00	10^4	0.00	0.00	0.00	0.00	0.00	0.00	0.00	0.00
1A	9.4964	-5.23	10^4	-5.67	2.48	-0.44	-0.34	0.42	-0.265	0.12	-0.035
1B	9.4964	-7.87	10^4	-1.08	-2.48	1.87	-0.34	-0.33	0.265	-0.06	-0.035
2A	9.4964	7.87	10^4	1.08	-2.48	-1.87	-0.34	0.33	0.265	0.06	-0.035
2B	9.4964	5.21	10^4	5.67	2.48	0.44	-0.34	-0.42	-0.265	-0.12	-0.035
3A	9.4964	5.23	10^4	5.67	2.48	0.44	-0.34	-0.42	-0.265	-0.12	-0.035
3B	9.4964	7.87	10^4	1.08	-2.48	-1.87	-0.34	0.33	0.265	0.06	-0.035
4A	9.4964	-7.86	10^4	-1.08	-2.48	1.87	-0.34	-0.33	0.265	-0.06	-0.035
4B	9.4964	-5.23	10^4	-5.67	2.48	-0.44	-0.34	0.42	-0.265	0.12	-0.035
ALL	9.5484	0.00	10^4	0.00	0.00	0.00	-2.70	0.00	0.00	0.00	-0.30

Table 5.2.3: Computed low field change in harmonics caused by 4.57 mm (0.180") thick magnetic tuning shims at the given location, LOC, (see Fig. 5.2.1). The transfer function is given in T/m/kA.

LOC	δTF	δa_0	δa_1	δa_2	δa_3	δa_4	δa_5	δa_6	δa_7	δa_8	δa_9
None	0.000	0.00	0.00	0.00	0.00	0.00	0.00	0.00	0.00	0.00	0.00
1A	0.0119	12.30	-4.86	-2.09	4.05	-2.99	1.46	-0.44	-0.01	0.11	-0.09
1B	0.0119	8.43	4.85	-8.86	4.05	0.47	-1.46	0.70	-0.01	-0.17	0.09
2A	0.0119	8.43	-4.85	-8.86	-4.05	0.47	1.46	0.70	0.01	-0.17	-0.09
2B	0.0119	12.30	4.85	-2.09	-4.05	-2.99	-1.46	-0.44	0.01	0.11	0.09
3A	0.0119	-12.30	-4.85	2.09	4.05	2.99	1.46	0.44	-0.01	-0.11	-0.09
3B	0.0119	-8.43	4.85	8.86	4.05	-0.47	-1.46	-0.70	-0.01	0.17	0.09
4A	0.0119	-8.44	-4.85	8.86	-4.05	-0.47	1.46	-0.70	0.01	0.17	-0.09
4B	0.0119	-12.31	4.85	2.09	-4.05	2.99	-1.46	0.44	0.01	-0.11	0.09
ALL	0.0947	0.00	0.00	0.00	0.00	0.00	0.00	0.00	0.00	0.00	0.00
LOC	TF	δb_0	b_1	δb_2	δb_3	δb_4	δb_5	δb_6	δb_7	δb_8	δb_9
None	9.4889	0.00	10^4	0.00	0.00	0.00	0.00	0.00	0.00	0.00	0.00
1A	9.5008	-8.44	10^4	-8.86	3.68	-0.47	-0.670	0.70	-0.42	0.173	-0.04
1B	9.5008	-12.30	10^4	-2.09	-3.68	2.99	-0.669	-0.44	0.42	-0.115	-0.04
2A	9.5008	12.29	10^4	2.09	-3.68	-2.99	-0.668	0.44	0.42	0.115	-0.04
2B	9.5008	8.43	10^4	8.86	3.68	0.47	-0.671	-0.70	-0.42	-0.173	-0.04
3A	9.5008	8.43	10^4	8.86	3.68	0.47	-0.672	-0.70	-0.42	-0.173	-0.04
3B	9.5008	12.30	10^4	2.09	-3.68	-2.99	-0.670	0.44	0.42	0.113	-0.04
4A	9.5008	-12.31	10^4	-2.09	-3.68	2.99	-0.673	-0.44	0.42	-0.114	-0.04
4B	9.5008	-8.43	10^4	-8.86	3.68	-0.47	-0.671	0.70	-0.42	0.172	-0.04
ALL	9.5837	0.00	10^4	0.00	0.00	0.00	-5.28	0.00	0.001	0.00	-0.34

Table 5.2.4: Computed low field change in harmonics caused by 6.10 mm (0.240") thick magnetic tuning shims at the given location, LOC, (see Fig. 5.2.1). The transfer function is given in T/m/kA.

LOC	δTF	δa_0	δa_1	δa_2	δa_3	δa_4	δa_5	δa_6	δa_7	δa_8	δa_9
NONE	0.000	0.00	0.00	0.00	0.00	0.00	0.00	0.00	0.00	0.00	0.00
1A	0.0165	16.65	-6.13	-3.39	5.82	-4.11	1.89	-0.49	-0.08	0.18	-0.13
1B	0.0165	11.78	6.13	-11.97	5.82	0.33	-1.89	1.01	-0.08	-0.21	0.13
2A	0.0165	11.77	-6.13	-11.97	-5.82	0.33	1.89	1.01	0.08	-0.21	-0.13
2B	0.0165	16.64	6.13	-3.39	-5.82	-4.11	-1.89	-0.49	0.08	0.18	0.13
3A	0.0165	-16.65	-6.13	3.39	5.82	4.11	1.89	0.49	-0.08	-0.18	-0.13
3B	0.0165	-11.78	6.14	11.97	5.82	-0.33	-1.89	-1.01	-0.08	0.21	0.13
4A	0.0165	-11.79	-6.14	11.97	-5.82	-0.33	1.89	-1.01	0.08	0.21	-0.13
4B	0.0165	-16.67	6.13	3.39	-5.82	4.11	-1.89	0.49	0.08	-0.18	0.13
ALL	0.1304	-0.03	0.01	0.00	0.00	0.00	0.00	0.00	0.00	0.00	0.00
LOC	TF	δb_0	b_1	δb_2	δb_3	δb_4	δb_5	δb_6	δb_7	δb_8	δb_9
None	9.4889	0.00	10^4	0.00	0.00	0.00	0.00	0.00	0.00	0.00	0.00
1A	9.5054	-11.78	10^4	-11.97	4.69	-0.33	-1.08	1.01	-0.56	0.21	-0.04
1B	9.5054	-16.66	10^4	-3.39	-4.69	4.11	-1.08	-0.49	0.56	-0.18	-0.04
2A	9.5054	16.65	10^4	3.39	-4.69	-4.11	-1.08	0.49	0.56	0.18	-0.04
2B	9.5054	11.77	10^4	11.97	4.69	0.33	-1.08	-1.01	-0.56	-0.21	-0.04
3A	9.5054	11.78	10^4	11.97	4.69	0.33	-1.08	-1.01	-0.56	-0.21	-0.04
3B	9.5054	16.66	10^4	3.39	-4.69	-4.11	-1.08	0.49	0.56	0.18	-0.04
4A	9.5054	-16.66	10^4	-3.39	-4.69	4.11	-1.08	-0.49	0.56	-0.18	-0.04
4B	9.5054	-11.79	10^4	-11.97	4.69	-0.33	-1.08	1.01	-0.56	0.21	-0.04
ALL	9.6193	-0.03	10^4	0.00	0.00	0.00	-8.48	0.00	0.00	0.00	-0.30

In Table 5.2.5, the maximum possible correction is listed for the given thickness of tuning shims. In this case the thickness of a tuning shim is computed from the nominal value thickness of tuning shim; so that it can have either a negative or a positive value. In these calculations the magnitude of the shim thickness is the same at all eight locations (for example, it could be four tuning shims with 2 mm and the other four with -2 mm). For most (but not all) the change in harmonic is symmetric with respect to the sign of the tuning shim thickness. This means that in most cases if “+x” mm thick gives $+b_n$ change in harmonics then “-x” mm gives $-b_n$ change. However, the most notable exceptions are b_5 and b_9 . The non-linearity in these harmonics is associated with the non-linearity of the trigonometric expressions ($\Delta\theta$ in Eqs. (5.2.10)) at these angles. It may be emphasized that this is the maximum possible correction. The actual value of the harmonics produced by these shims would have an opposite sign to the measured harmonics. The computed maximum corrections, thus obtained, are given in Fig. 5.2.3 for the skew and normal sextupole (a_2 and b_2), skew and normal octupole (a_3 and b_3), skew and normal decapole (a_4 and b_4) harmonics. In Fig. 5.2.4 they are given for the skew and normal do-decapole (a_5 and b_5) harmonics and in Fig. 5.2.5 for a_9 and b_9 harmonics.

Table 5.2.5: Maximum possible low field correction in the harmonics as a function of shim thickness (T) in mm as measured from the nominal value of 3.05 mm (0.012") iron. The shim thickness can be either negative or positive. The change in transfer function (δTF) is given in T/m/kA.

T(mm)	δTF	δa_0	δa_1	δa_2	δa_3	δa_4	δa_5	δa_6	δa_7	δa_8	δa_9
-3.05	0.0722	56.85	24.54	30.74	23.24	8.87	7.576	3.004	-0.324	0.792	0.521
-2.54	0.0601	48.24	21.02	26.07	19.65	7.60	6.497	2.572	-0.246	0.682	0.452
-2.03	0.0474	39.18	17.16	21.12	15.92	6.22	5.318	2.106	-0.190	0.558	0.368
-1.52	0.0354	29.62	13.01	15.99	12.04	4.73	4.048	1.600	-0.033	0.426	0.281
-1.02	0.0234	19.93	8.79	10.74	8.10	3.19	2.736	1.085	0.094	0.288	0.193
-0.51	0.0114	10.0	4.42	5.38	4.05	1.59	1.374	0.547	0.047	0.146	0.096
0.0	0.0	0.0	0.0	0.0	0.0	0.0	0.0	0.0	0.0	0.0	0.0
0.51	-0.0118	-9.94	-4.38	-5.39	-4.08	-1.62	-1.372	-0.538	-0.045	-0.136	-0.094
1.02	-0.0228	-19.93	-8.78	-10.72	-8.12	-3.19	-2.730	-1.077	-0.092	-0.284	-0.190
1.52	-0.0334	-29.62	-13.01	-15.97	-12.09	-4.74	-4.039	-1.599	-0.137	-0.419	-0.281
2.03	-0.0430	-39.16	-17.14	-21.12	-15.97	-6.23	-5.308	-2.102	-0.190	-0.549	-0.366
2.54	-0.0519	-48.25	-21.00	-26.04	-19.71	-6.38	-6.490	-2.564	-0.246	-0.670	-0.448
3.05	-0.0598	-56.88	-24.52	-30.72	-23.28	-7.57	-7.575	-2.987	-0.324	-0.784	-0.524
T(mm)	δTF	δb_0	b_1	δb_2	δb_3	δb_4	δb_5	δb_6	δb_7	δb_8	δb_9
-3.05	0.0720	56.87	10^4	30.73	18.78	8.87	2.726	2.988	2.236	0.786	0.286
-2.54	0.0600	48.28	10^4	26.03	16.11	7.60	2.497	2.562	1.911	0.669	0.238
-2.03	0.0479	39.19	10^4	21.12	13.15	6.22	2.193	2.103	1.573	0.552	0.184
-1.52	0.0352	29.63	10^4	15.98	10.0	4.72	1.796	1.602	1.193	0.417	0.127
-1.02	0.0232	19.92	10^4	10.75	6.76	3.18	1.295	1.076	0.808	0.284	0.081
-0.51	0.0112	10.01	10^4	5.38	3.38	1.60	0.695	0.538	0.407	0.142	0.036
0.0	0.0	0.0	10^4	0.0	0.0	0.0	0.0	0.0	0.0	0.0	0.0
0.51	-0.0114	-9.96	10^4	-5.37	-3.38	-1.61	-0.795	-0.551	-0.400	-0.146	-0.029
1.02	-0.0225	-19.91	10^4	-10.72	-6.73	-3.20	-1.665	-1.093	-0.805	-0.284	-0.047
1.52	-0.0328	-29.63	10^4	-15.97	-9.98	-4.72	-2.638	-1.610	-1.188	-0.423	-0.053
2.03	-0.0432	-39.14	10^4	-21.12	-13.14	-6.22	-3.679	-2.107	-1.564	-0.553	-0.051
2.54	-0.0520	-48.27	10^4	-26.00	-16.06	-6.40	-4.789	-2.582	-1.917	-0.671	-0.041
3.05	-0.0598	-56.88	10^4	-30.71	-18.78	-7.56	-5.962	-3.008	-2.225	-0.785	-0.012

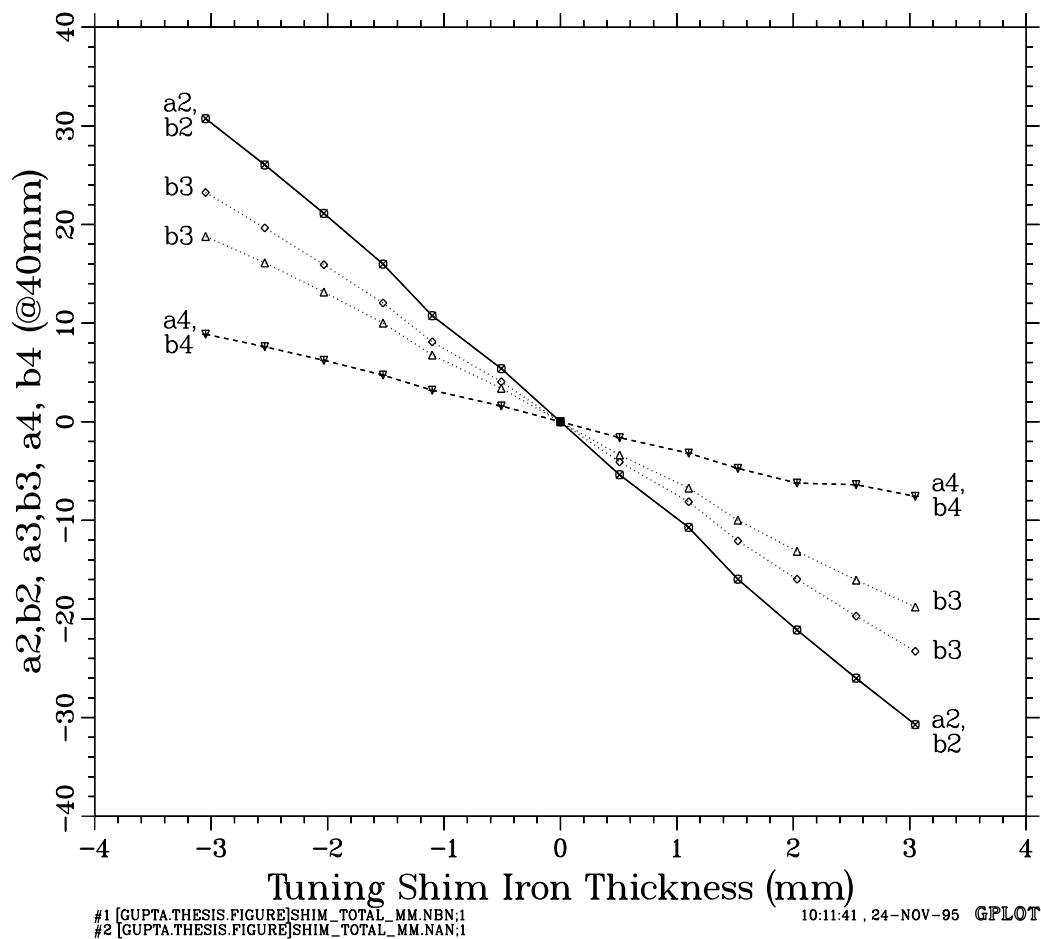


Figure 5.2.3: The computed maximum possible low field correction in the skew and normal sextupole (a_2 and b_2), the skew and normal octupole (a_3 and b_3), and the skew and normal decapole (a_4 and b_4) harmonics as a function of tuning shim thickness (1mil = 0.0254 mm). The tuning shim thickness is measured from its nominal value and therefore has both negative and positive values.

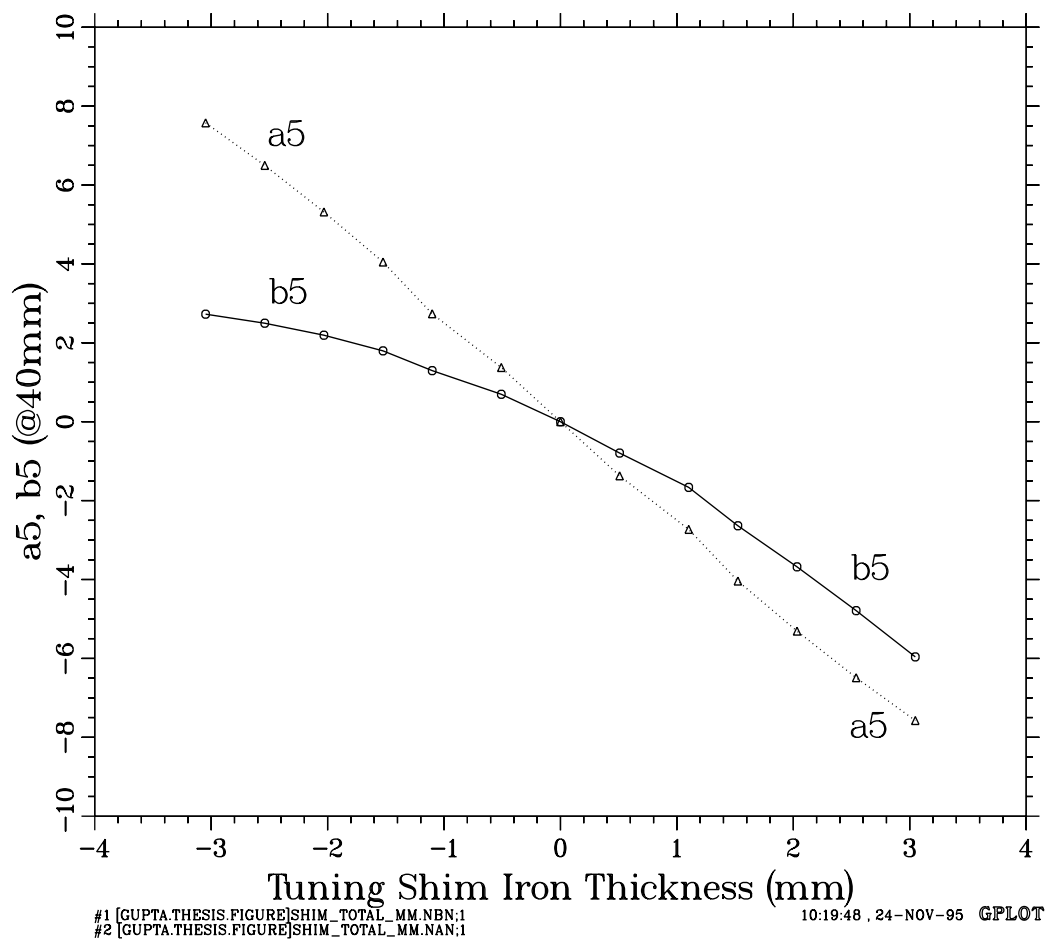


Figure 5.2.4: The computed maximum possible low field correction in the skew and normal do-decapole (a_5 and b_5) harmonics as a function of tuning shim thickness (1mil = 0.0254 mm). The tuning shim thickness is measured from its nominal value and therefore has both negative and positive values.

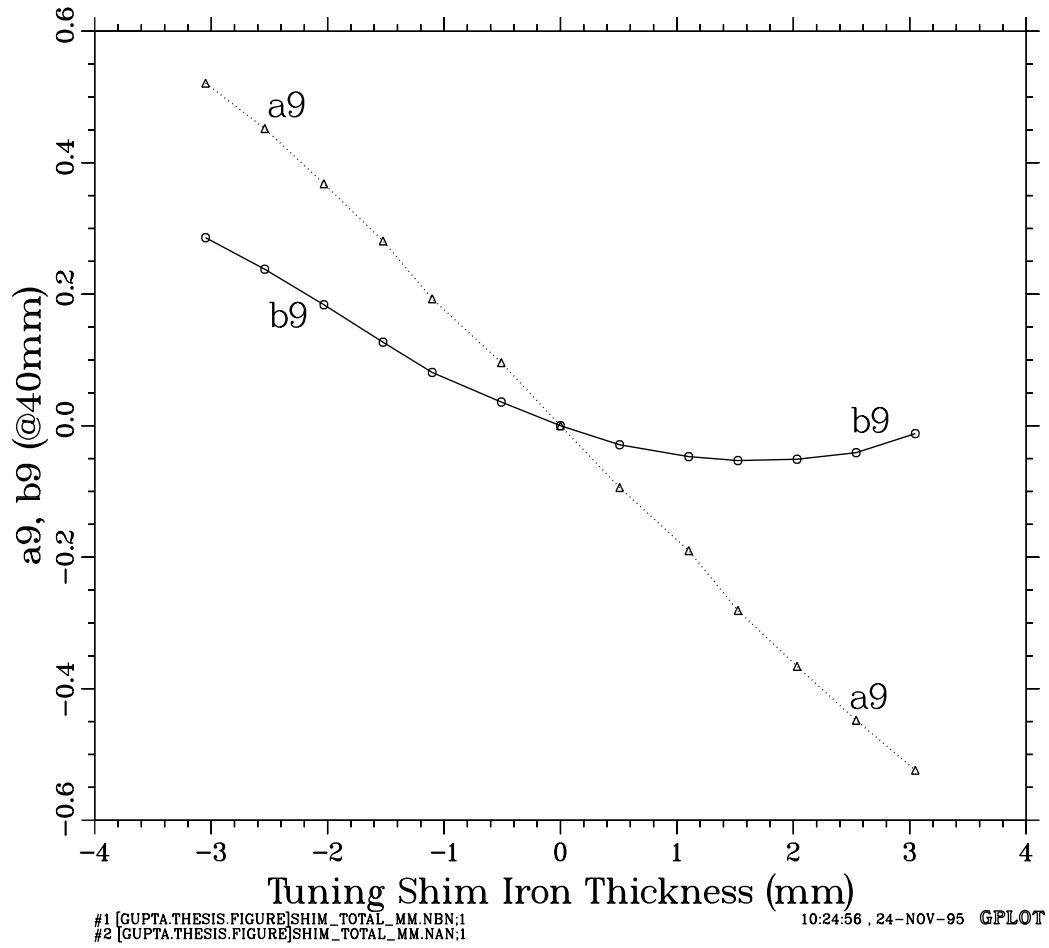


Figure 5.2.5: The computed maximum possible low field correction in the a_9 and b_9 harmonics as a function of tuning shim thickness (1mil = 0.0254 mm). The tuning shim thickness is measured from its nominal value and therefore has both negative and positive values.

5.2.4.3. Numerical Calculations for High Field Correction

At high field, the magnetization of the shims become almost constant, so their contribution to the harmonics decreases with increasing field. In this case the correction in the field harmonics produced by the tuning shim is smaller by an amount that depends on the current. The absolute loss in correction depends on the harmonic concerned and may also depend on the details of the tuning shim configuration. Since the maximum beam luminosity in RHIC is desired at the top energy, the tuning shim correction is optimized for the design current of 5 kA. This means that generally there will be an over-correction at low field.

The current dependence of the harmonic correction for particular locations of tuning shim is examined in Table 5.2.6 for the skew harmonics and Table 5.2.7 for the normal harmonics. These calculations are for the change in harmonics created by the nominal size (3.175 mm) tuning shim compared to the no-shim case. In these tables, the second row shows the location of the tuning shim for which the current dependence in the harmonic in the first row is given. This is one of the several locations where that particular harmonic has the maximum positive value. The last row shows the ratio of correction between 1 kA and 5 kA for each harmonic. This is the over-correction factor at low current when the measured harmonics are compensated at 5 kA. The error in harmonic calculations is typically of the order of 0.01 unit for higher order harmonics (b_5/a_5 and higher) and 0.1 unit in lower order harmonics. Therefore a_7 and b_9 harmonics, which have small values, will have a relatively large error, and the significantly different value of “1kA/5kA” (last row in Table 5.2.6) is not real.

The current dependence of the change in the harmonics produced by shims can also be seen in Fig. 5.2.6 and Fig. 5.2.7. Here the ratio of the shim correction at any current to that at 1 kA is plotted for the same location as those given in Table 5.2.6 and Table 5.2.7. At 5 kA this number is the inverse of the number given in the last row of the above tables.

The influence of this saturation on the maximum tuning shim correction range is examined here for each harmonic. Maximum range is obtained when, for each individual harmonic, all shims are put in a configuration which gives the maximum change. This is shown in Table 5.2.8. To obtain the range (i.e. maximum positive or maximum negative correction) each individual shim is either made of all iron (magnetic) laminations or all brass laminations (non-magnetic). The correction is computed at low current (1kA) and at the maximum design current (5kA). The ratio, which represent the amount of over-correction

at low field, is also computed here. The significantly different values of ratio for a_7 and b_9 harmonics are not real, as explained earlier.

Table 5.2.6: The current dependence of the change in skew harmonics generated by a nominal tuning shim at the location (listed below) which gives the maximum positive correction compared to the no-shim case. The relative computational error in a_7 is large and the increase at 5 kA is artificial because of its smaller value.

Current (kA)	a_0 (1A)	a_1 (1B)	a_2 (3B)	a_3 (1B)	a_4 (3A)	a_5 (1A)	a_6 (1B)	a_7 (1B)	a_8 (3B)	a_9 (1B)
0.0	7.88	3.32	5.673	2.428	1.874	0.963	0.414	0.026	0.12	0.055
1.0	7.87	3.31	5.67	2.429	1.873	0.963	0.415	0.025	0.121	0.054
3.0	7.83	3.29	5.651	2.414	1.867	0.958	0.411	0.025	0.119	0.054
4.0	7.51	3.16	5.442	2.281	1.79	0.913	0.384	0.028	0.115	0.051
4.5	7.24	3.07	5.217	2.169	1.706	0.871	0.358	0.034	0.109	0.046
5.0	6.94	2.97	4.948	2.035	1.584	0.826	0.327	0.039	0.103	0.041
5.5	6.49	2.75	4.578	1.898	1.457	0.749	0.293	0.038	0.093	0.036
6.0	5.83	2.38	4.039	1.735	1.279	0.649	0.259	0.029	0.079	0.031
7.0	4.43	1.76	3.055	1.386	0.992	0.493	0.204	0.019	0.061	0.024
8.0	3.59	1.46	2.506	1.171	0.834	0.411	0.176	0.013	0.051	0.021
1kA/5kA	1.13	1.11	1.15	1.19	1.18	1.17	1.27	0.64*	1.17	1.32

*This ratio contains large errors due to smaller values of a_7

Table 5.2.7: The current dependence of the change in normal harmonics generated by a nominal tuning shim at the location (listed below) which gives the maximum positive correction compared to the no-shim case.

Current (kA)	b_0 (2A)	$\delta(TF)$ (ALL)	b_2 (2B)	b_3 (1A)	b_4 (1B)	b_5 (ALL)	b_6 (1A)	b_7 (1B)	b_8 (1A)	b_9 (ALL)
0.0	7.87	0.0075	5.656	2.482	1.87	-0.342	0.416	0.265	0.119	-0.037
1.0	7.87	0.0074	5.655	2.482	1.868	-0.341	0.416	0.266	0.12	-0.037
3.0	7.84	0.0074	5.639	2.468	1.859	-0.338	0.413	0.264	0.119	-0.038
4.0	7.58	0.0071	5.451	2.366	1.759	-0.31	0.386	0.248	0.114	-0.037
4.5	7.31	0.0068	5.162	2.276	1.676	-0.283	0.361	0.235	0.108	-0.035
5.0	6.99	0.0064	4.917	2.182	1.575	-0.248	0.33	0.218	0.102	-0.034
5.5	6.52	0.006	4.552	1.999	1.445	-0.225	0.298	0.195	0.092	-0.031
6.0	5.81	0.0054	4.051	1.73	1.277	-0.212	0.263	0.168	0.078	-0.026
7.0	4.44	0.004	3.053	1.285	0.984	-0.175	0.207	0.131	0.061	-0.02
8.0	3.63	0.0032	2.492	1.058	0.827	-0.155	0.178	0.111	0.05	-0.018
1kA/5kA	1.13	1.16	1.15	1.14	1.19	1.37	1.26	1.22	1.18	1.09

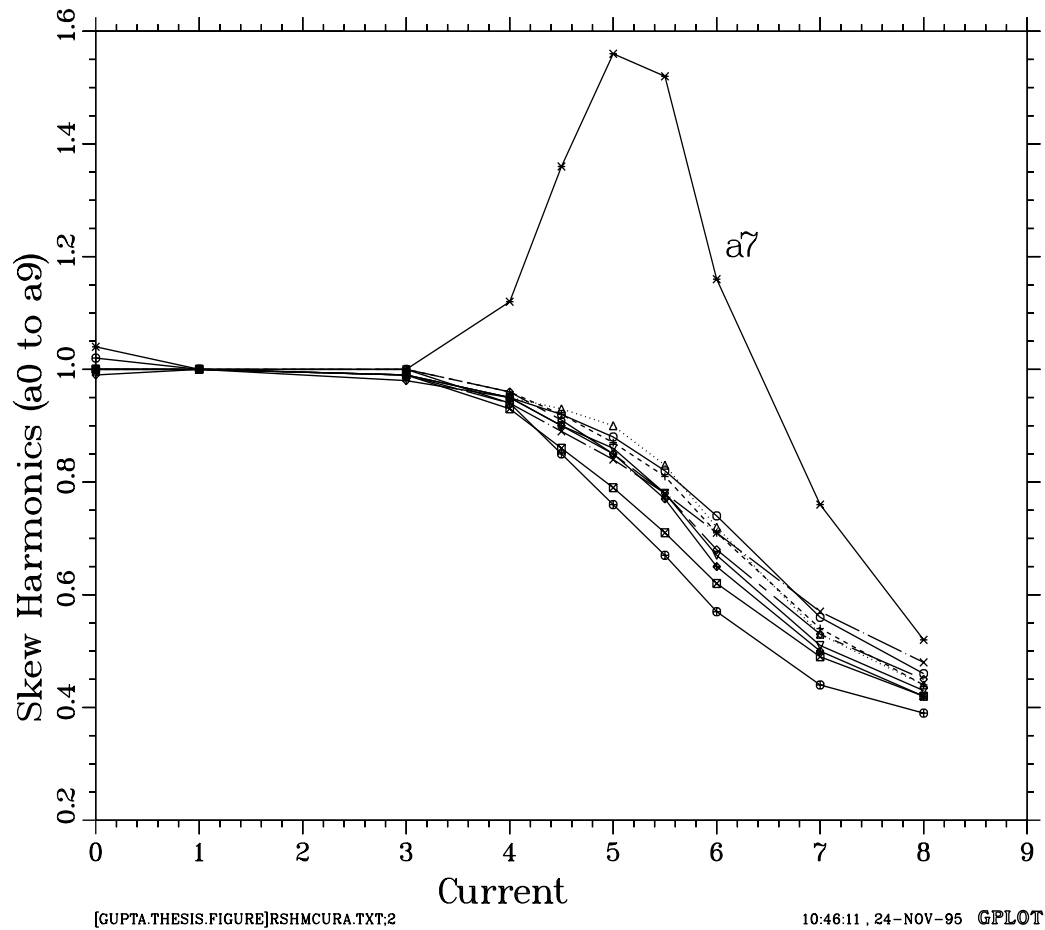
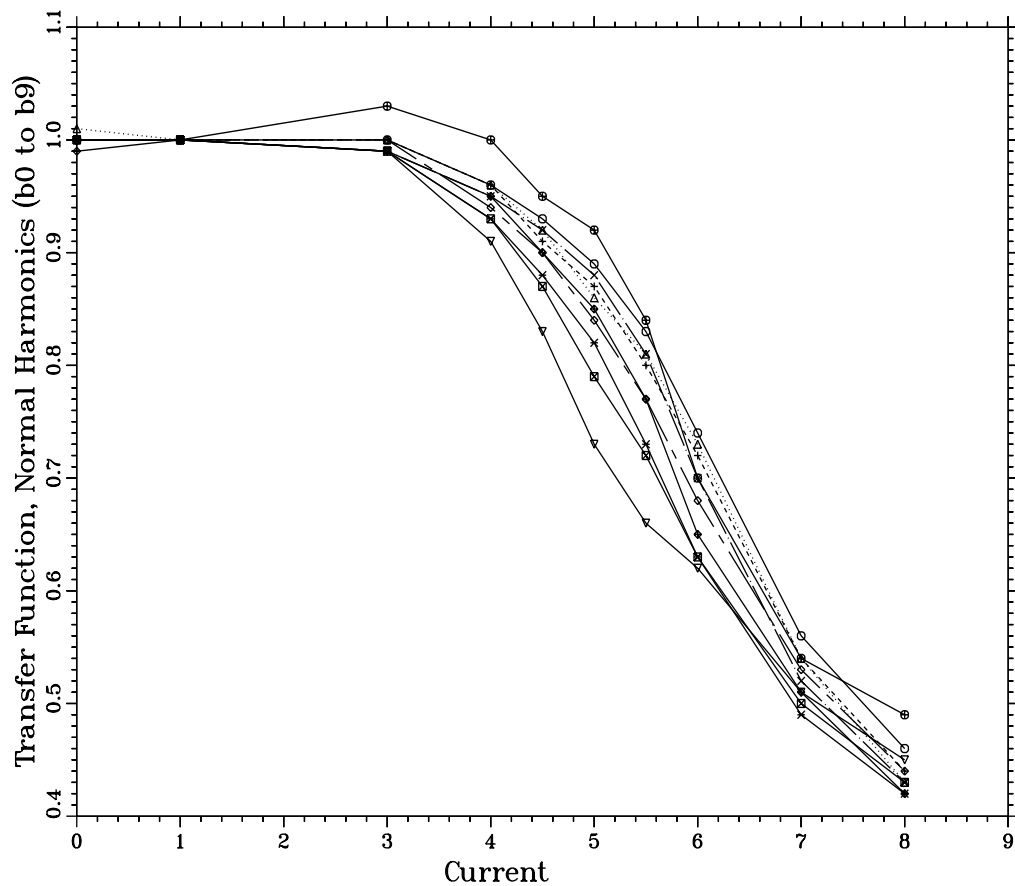


Figure 5.2.6: The ratio of the harmonics generated by a tuning shim at the given current to those at 1 kA. The design current is 5 kA. The shim location is that which gives the maximum correction in the harmonics produced by tuning shims having the nominal thickness.



[GUPTA.THESIS.FIGURE]RSHMCURB.TXT:2

10:47:57, 24-NOV-95 G PLOT

Figure 5.2.7: The ratio of the harmonics generated by a tuning shim at the given current to those at 1 kA. The design current is 5 kA. The shim location is that which gives the maximum correction in the harmonics produced by tuning shims having the nominal thickness.

Table 5.2.8: The maximum possible change in harmonics (range) which can be made by tuning shims in the RHIC 130 mm aperture insertion quadrupoles. To obtain this number for each harmonic, each of eight tuning shims has either a maximum (all) or minimum (none) iron content so that the contributions add. The values are computed at low current (1 kA) and at the nominal design current (5 kA). Since the correction is made at 5kA, the ratios $A_{1kA/5kA}$ and $B_{1kA/5kA}$ indicate the over-correction factor at low current. The transfer function is given in T/m/kA and harmonics are given at a reference radius of 40 mm.

Harm a_n	Correction (Range) $_{1kA}$	Correction (Range) $_{5kA}$	Ratio $_{an}$ $A_{1kA/5kA}$	Harm b_n	Correction (Range) $_{1kA}$	Correction (Range) $_{5kA}$	Ratio $_{bn}$ $B_{1kA/5kA}$
a_0	113.73	91.82	1.239	b_0	113.75	91.89	1.238
a_1	49.06	40.96	1.198	TF	0.132	0.1047	1.261
a_2	61.464	48.505	1.267	b_2	61.439	48.372	1.270
a_3	46.525	36.104	1.289	b_3	37.557	30.832	1.218
a_4	17.754	14.41	1.232	b_4	17.745	14.433	1.229
a_5	15.151	12.148	1.247	b_5	8.688	6.099	1.424
a_6	5.991	4.724	1.268	b_6	5.996	4.734	1.267
a_7	0.645	0.196	3.291	b_7	4.461	3.444	1.295
a_8	1.576	1.188	1.327	b_8	1.571	1.18	1.331
a_9	1.045	0.766	1.364	b_9	0.298	0.304	0.980
a_{10}	0.329	0.232	1.418	b_{10}	0.328	0.235	1.396
a_{11}	0.159	0.135	1.178	b_{11}	0.192	0.129	1.488
a_{12}	0.066	0.052	1.269	b_{12}	0.068	0.054	1.259
a_{13}	0.0243	0.0137	1.774	b_{13}	0.0418	0.0316	1.323

5.2.5. Symmetries in the Harmonics Generated by Tuning Shims

The harmonics generated by the same tuning shim placed at two different locations follow certain symmetries or anti-symmetries. This means that the harmonics created by a same size (iron content) tuning shim placed in a certain pair of locations have the same magnitude. These two locations are called symmetric with respect to a particular harmonic if the sign of the harmonic change is the same and anti-symmetric if the sign is opposite.

The following rules are obtained for quadrupoles from Eqs. (5.2.10) or Eqs. (5.2.11).

If these two locations are left and right with respect to the vertical axis (for example see locations 1A and 2B in Fig. 5.2.1), then the odd b_n and even a_n are symmetric and even b_n and odd a_n are anti-symmetric. This means that $b_3(@1A) = b_3(@2B)$ and $a_3(@1A) = -a_3(@2B)$.

Similarly if these two locations are top and bottom (for example locations 1A and 4B), then all b_n are symmetric and all a_n are anti-symmetric.

The remaining combination is of two locations that are on the two sides of the coil pole (for example locations (1A,1B), (2A,2B), etc.) If a relationship in the harmonics generated between these two locations is obtained, then the harmonics created by a tuning shim at one location completely determines the value of harmonics at all other locations. In this case, as explained below, the symmetries in the harmonics are somewhat complicated.

In the case of odd harmonics, two locations are symmetric for harmonics b_{4k+1} and a_{4k+3} for $k=0,1,2,\dots$ (for example $b_5(@1A) = b_5(@1B)$ or $a_3(@3A) = a_3(@3B)$) and two locations are anti-symmetric for harmonics b_{4k+3} and a_{4k+1} (for example $b_3(@2A) = -b_3(@2B)$). Even harmonics have a cross relationship between the normal and skew components b_n and a_n as follows : (a) the harmonics b_{4k+2} and a_{4k+2} are symmetric at location 1 and 3 (for example $b_2(@1A) = a_2(@1B)$) and are anti-symmetric at location 2 and 4 and (b) the harmonics b_{4k+4} and a_{4k+4} are anti-symmetric at location 1 and 3 and are symmetric at location 2 and 4 (for example $a_4(@4A) = b_4(@4B)$).

5.2.6. Independent and Coupled Changes in Harmonics Correction

A consequence of correcting field harmonics with tuning shims is the creation of other harmonics in the process. These other harmonics are those that are allowed by the symmetry of the shims. Therefore, “n” tuning shims can not fully compensate any arbitrary “n” harmonics.

In this design, eight tuning shims correct eight harmonics. The following three rules will apply in a quadrupole :

1. of eight harmonics, four must be skew (a_n) and four must be normal (b_n),
2. of the four skew and four normal harmonics, two must be odd (e.g. a_3) and two must be even (e.g. b_4)
3. for any change in an odd harmonic $n=2k+1$, with $k=0,1,2,..$ the harmonic $n=2k+5$ will also change, e.g. a change in b_3 will cause a coupled change in b_7 , as well.

Despite the above restrictions, the desired eight harmonics (a_2, a_3, a_4, a_5) and (b_2, b_3, b_4, b_5) can be independently minimized. Though the change in the other harmonics is determined by the coupling, certain couplings can be minimized in the initial yoke design by properly choosing the azimuthal locations of the tuning shims. For example, the coupling of b_5 to b_9 is small when the tuning shims are positioned anywhere within the range $\theta = 30^\circ$ to $\theta = 35^\circ$ (the range is fixed in the original design and can not be changed during the tuning process). In an optimized scheme the coupling in most harmonics should generally be an order of magnitude smaller than the primary harmonics. (Please refer to Table 5.2.5).

5.2.7. Comparison with the Measurements

Calculations are now compared with measurements of the field harmonics produced by magnetic shims. The calculations, as described in the previous section, are performed with the code POISSON. The comparison is made first in the low current case. In this case the permeability of the iron is assumed to be infinite. The low current measurements are made at room temperature (warm) when the magnet is not in a superconducting state; the current is carried by the copper fraction of the superconducting cable. In the following discussion, the shim thickness means the thickness of the low carbon steel (magnetic iron) in the tuning shim package. As mentioned earlier, the actual thickness of the package is

constant since the rest of the space is filled by non-magnetic brass. In the calculations, the shim thickness is varied in steps of 0.51 mm (0.020") and in the measurements in steps of 1.52 mm (0.060"). The change in harmonic (or harmonic due to the tuning shim) is obtained by subtracting out the harmonic of the no-shim case from the harmonic of the given shim thickness case. In Fig. 5.2.8, calculations and measurements of the skew and normal sextupole, the skew and normal octupole, and the skew and normal decapole harmonics are compared. In Fig. 5.2.9, calculations and measurements of the a_6 , b_6 , a_7 , b_7 , a_8 and b_8 harmonics are compared. In Fig. 5.2.10, calculations and measurements of the transfer function (gradient), skew and normal dodecapole and the a_9 and b_9 harmonics are compared. In the case of the skew quadrupole harmonic, only calculations are given as this harmonic is not available with present measurement techniques. It may be mentioned that in addition to the field gradient (or transfer function), b_5 and b_9 are harmonics allowed by the quadrupole geometry.

Though the symbols (measurements) and type of lines (calculations) are difficult to resolve for individual shim locations in these figures, it has been observed that the measurements always lie on the top of the computed values for each tuning shim location. The difference between the calculations and measurements is quite small (<0.05). It is quite clear from these figures that there is good agreement between the calculations and measurements of the field harmonics produced by the tuning shims at low currents.

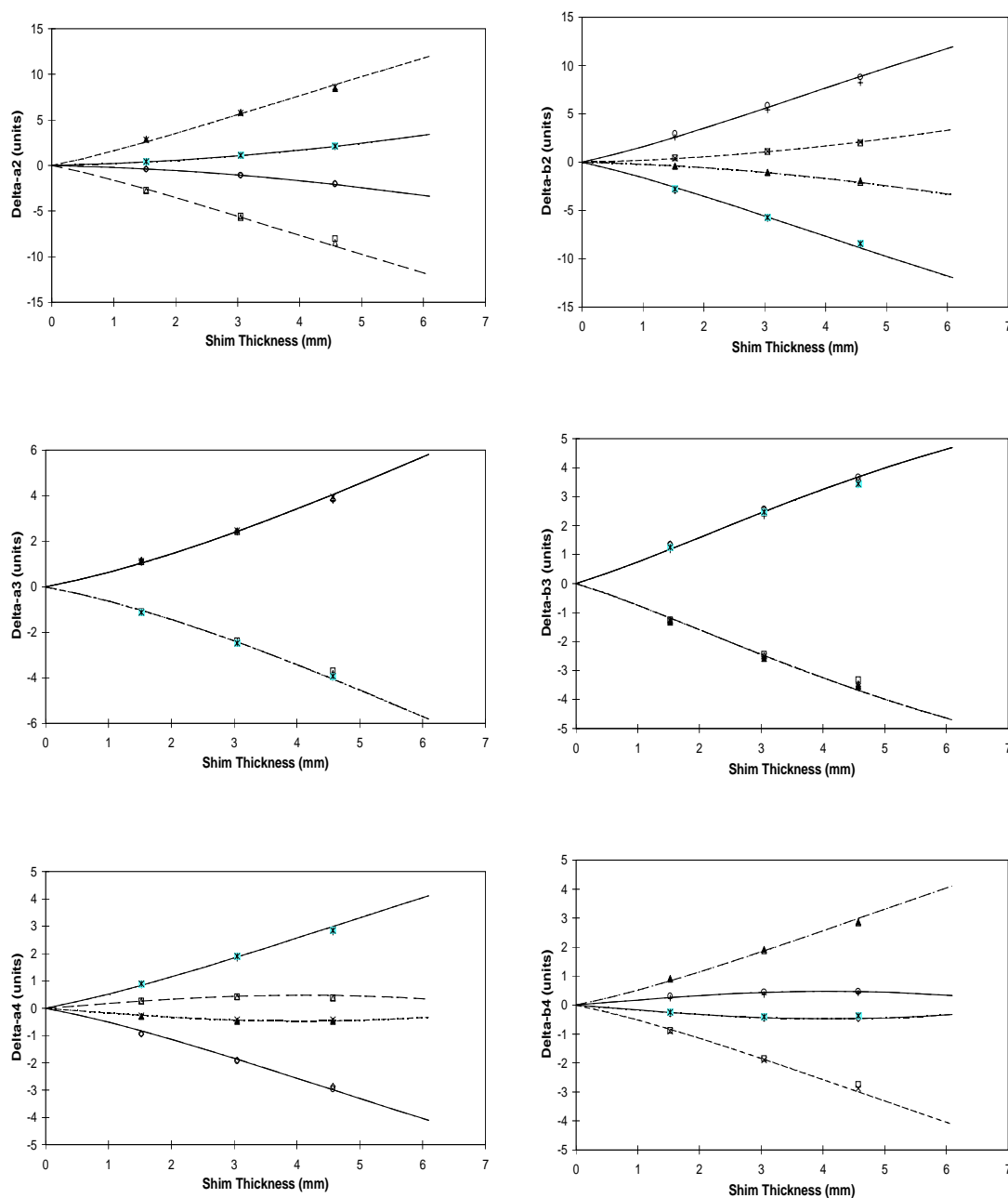


Figure 5.2.8: A comparison between calculations and measurements of the field harmonics created by the tuning shims at low fields. These are the changes in harmonics relative to the *no shim* or *zero shim* case for each shim. The eight symbols (see text) represent the measurements for the eight tuning shim locations and the eight lines (see text) are the calculations for these locations. The symbols and lines for the harmonics at two or four locations overlap as per the symmetries described in the previous section.

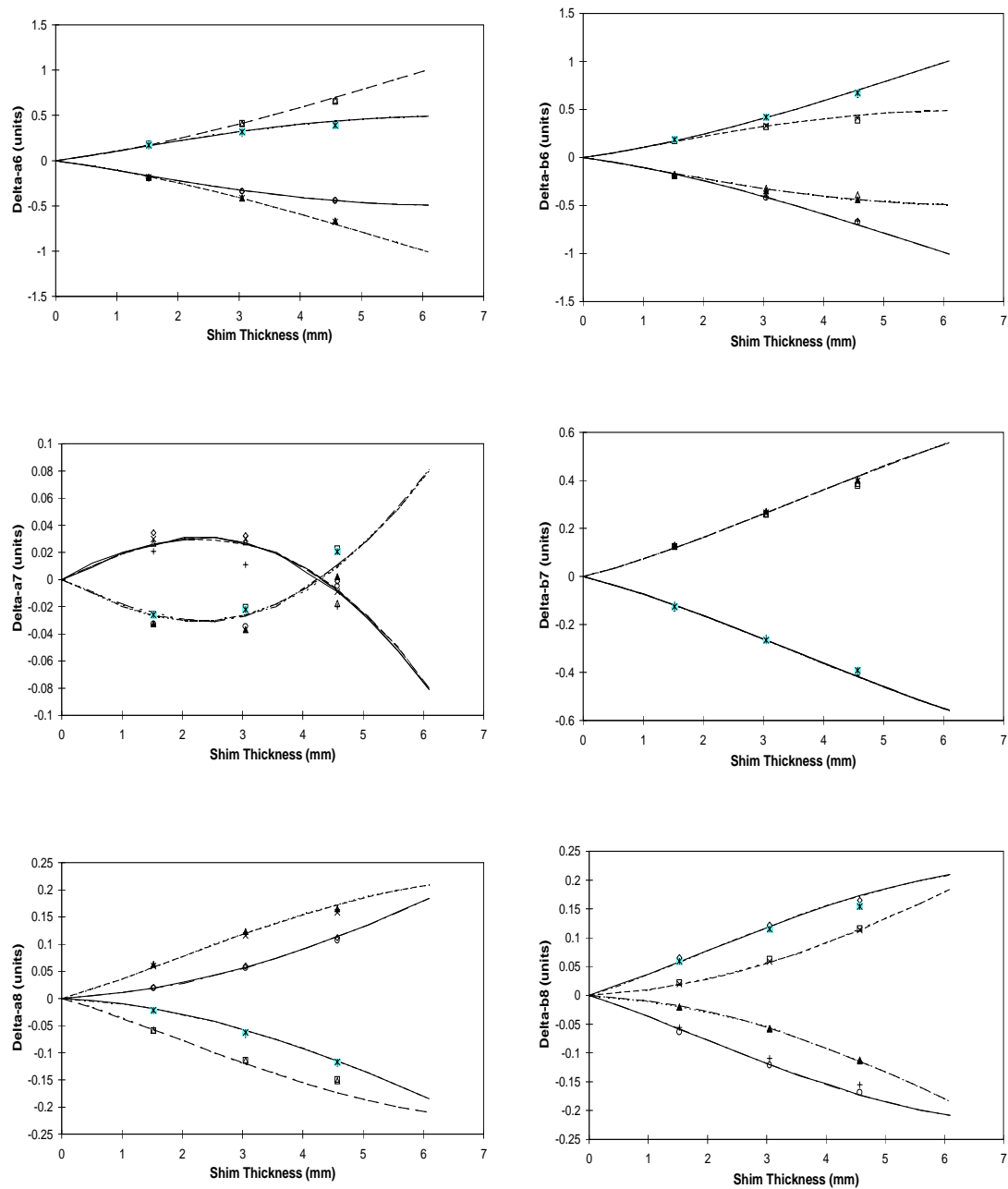


Figure 5.2.9: A comparison between calculations and measurements of the field harmonics created by the tuning shims at low fields. These are the changes in harmonics relative to the *no shim* or *zero shim* case for each shim. The eight symbols (see text) represent the measurements for the eight tuning shim locations and the eight lines (see text) are the calculations for these locations. The symbols and lines for the harmonics at two or four locations overlap as per the symmetries described in the previous section.

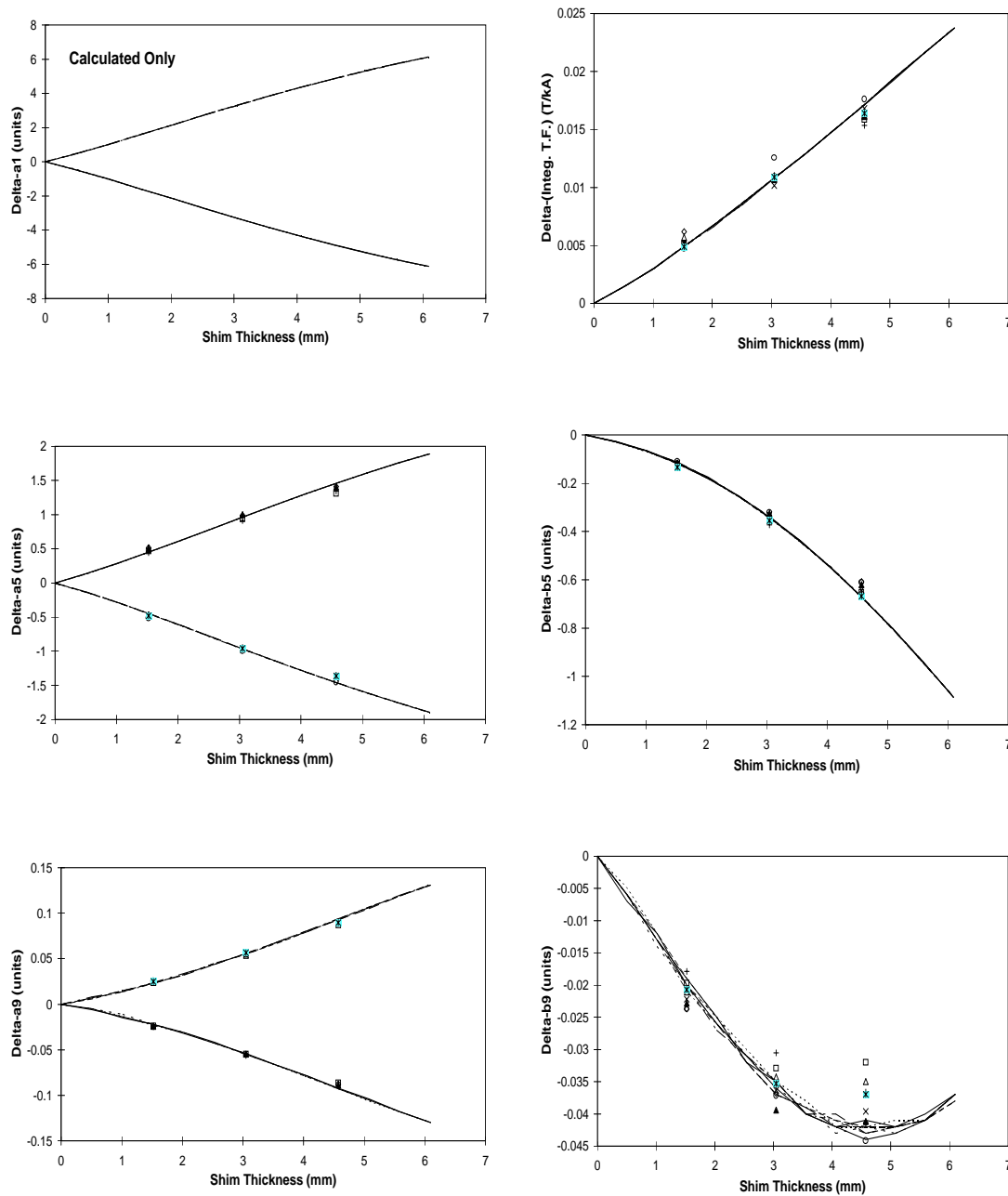


Figure 5.2.10: A comparison between calculations and measurements of the field harmonics created by the tuning shims at low fields. These are the changes in harmonics relative to the *no shim* or *zero shim* case for each shim. The eight symbols (see text) represent the measurements for the eight tuning shim locations and the eight lines (see text) are the calculations for these locations. The symbols and lines for the harmonics at two or four locations overlap as per the symmetries described in the previous section.

5.2.8. Tuning Shim Correction Vs. External Correctors

Harmonic errors in magnets are usually corrected by external corrector magnets. These give a lumped compensation to the beam dynamics of the distortion caused by the harmonic errors. These harmonic correctors are either located at the end of the magnet to correct for the errors in the individual magnets or they are lumped together and placed elsewhere in the machine. Valuable space for such correctors must be provided in the machine. External correctors provide the flexibility of adjustable correction by simply changing the current in the power supplies. However, they add to the component and power supply cost and complicate the machine operation. In order to independently correct eight harmonics one must have at least eight correction coils, either in one magnet or in a number of magnets.

In contrast, the tuning shim correction scheme corrects harmonic errors locally. The tuning shims require no extra space in the machine since they are installed inside each magnet. They are relatively inexpensive and require no external power supply to operate, which simplifies machine operation. Of course, there is no flexibility in the harmonic correction after the magnets are installed in the machine. However, the harmonics are measured after the tuning shims are inserted in each magnet and if the correction is not satisfactory they can immediately be adjusted.

The crucial advantage of the tuning shim scheme is its ability to correct errors locally. To explain this point, some basic considerations of beam optics in the RHIC interaction region (as set by accelerator physicists) are reviewed here together with the implications for field quality in the interaction region quadrupoles [171]. The variation in $\sqrt{\beta_x}$ and $\sqrt{\beta_y}$ ($\sqrt{\beta_x}$ and $\sqrt{\beta_y}$ are proportional to the horizontal and vertical beam size) in the interaction region optics is shown in Fig. 5.2.11. One can note a rapid variation in the beta function, particularly in the insertion triplets, which consist of three 130 mm aperture quadrupoles. As a result, lumped external correctors would not be able to fully compensate the effects of distributed errors in the magnets on the orbit [171]. The tuning shim scheme, which removes the errors in eight harmonics locally, is much more effective. A larger good field region in the magnet means that the beam can be squeezed to a smaller size at the crossing point resulting in a higher luminosity. In the RHIC interaction region quadrupoles 5σ of the beam is expected to use 71% of the coil aperture. With tuning shims, a large fraction of the physical aperture can be made a good field aperture.

The tuning shim scheme, though crucial in the interaction region quadrupoles, could also be used in a large scale production of magnets with limited harmonics. In that case,

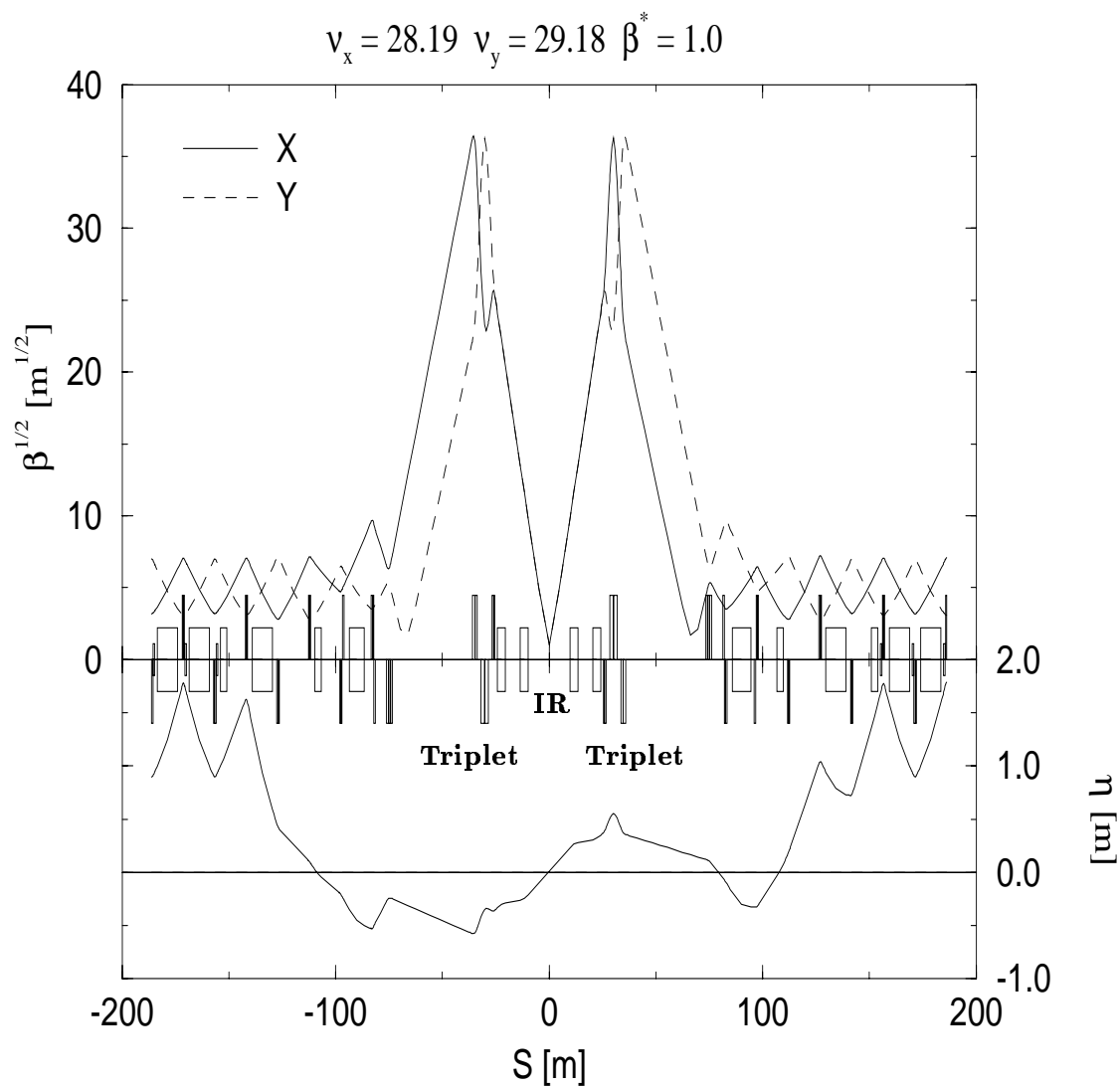


Figure 5.2.11: The variation in the square-root of the betatron functions (β_x , β_y) and dispersion function (η) in a RHIC insertion region for $\beta^* = 1.0$ (courtesy Jie Wei). The horizontal beam size is proportional to $\sqrt{\beta_x}$ and η and the vertical beam size is proportional to $\sqrt{\beta_y}$. A large beam size can be seen on the two sides of the insertion region (IR) where the focusing triplets are located.

it would be essential to further simplify the logistics of implementing such a scheme in an industrial environment. The use of this scheme was examined for SSC collider dipole magnets. The SSC magnets use stainless steel collars. In this case, it would perhaps be best to measure the harmonics before the collared coil is put in the yoke. The thickness of the magnetic material in the tuning shims would be determined by the measured harmonics in the collared coil in the absence of the yoke. The shims would be installed before (or during) the collared coil assembly into the yoke.

5.3. Tuning Yoke Length at Magnet Ends for Field Correction

Schemes are proposed here to correct deviations in the integral transfer function and the skew quadrupole harmonic in dipole magnets. As against the tuning shim scheme discussed earlier, the schemes proposed here are implemented only near the ends of the magnet. These schemes are based on adjusting the proportion of magnetic, low carbon steel to non-magnetic, stainless steel laminations to correct measured errors.

In the body (straight section) of the superconducting magnets, the yoke laminations (made of low carbon, magnetic steel) generally contribute 15% to 40% of the total field depending on the details of a particular design. The low carbon, magnetic steel laminations are replaced by non-magnetic, stainless steel laminations in the ends of the SSC and most other magnets, to reduce the maximum field on the conductor in an attempt to improve quench performance. However, this also reduces the integral field (or integral transfer function) of the magnet. In RHIC magnets (all except the design of the 180 mm aperture, insertion dipoles), the laminations in the ends are made of low carbon magnetic steel in order to maximize the integral transfer function. The proposed schemes of field adjustments are more powerful and natural to adopt in the former (SSC) type of magnet designs.

It is proposed here that while keeping the total physical length constant, the yoke magnetic length is adjusted to compensate for the following errors : (a) The total magnetic length (or the length of yoke laminations) can be adjusted to correct an error in the integral transfer function. (b) A deliberate up-down asymmetry in the magnetic yoke length between the top and bottom halves can be used to compensate for the measured skew quadrupole (a_1) harmonic. The proposed correction would take place towards the magnet ends as shown in Fig. 5.3.1. The starting of the actual location of the correction would be in the body (straight section) of the magnet where the local magnetic field is still high.

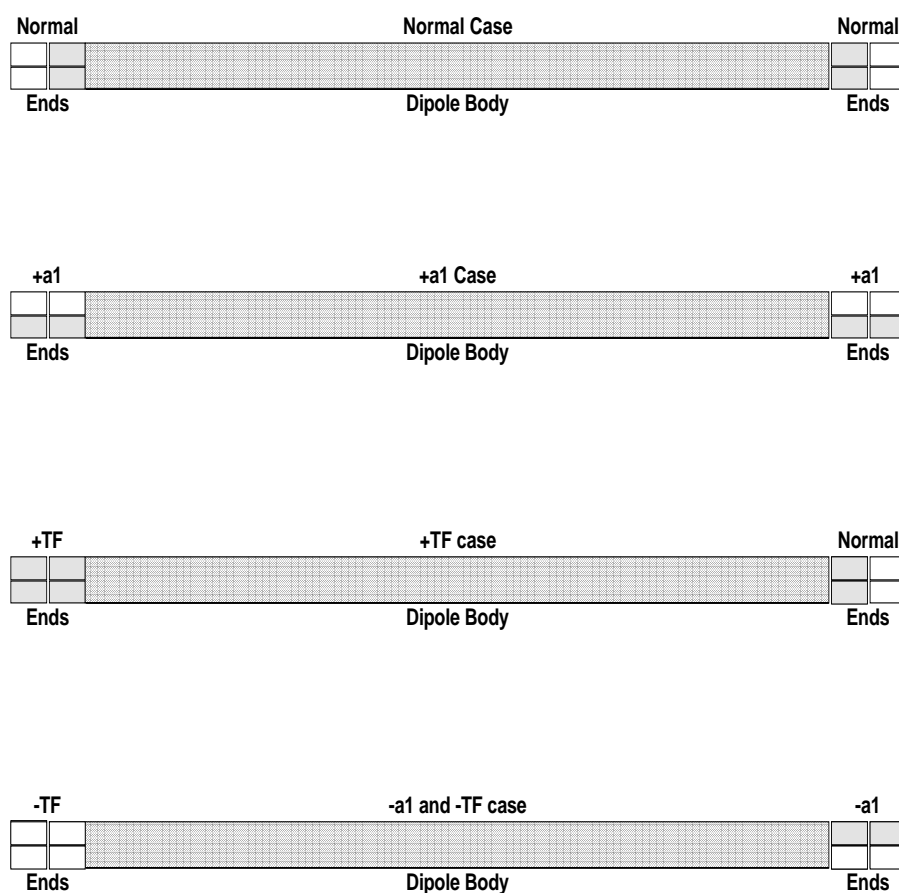


Figure 5.3.1: A conceptual diagram for correcting the integral a_1 harmonic and integral transfer function in a superconducting dipole magnet. The proposed adjustment is applied in the end region of the magnet. The actual starting point would be somewhere in the dipole body where the field is still high. In the normal case (top figure) the change between the magnetic, low carbon steel laminations [dark or filled] and non-magnetic stainless steel laminations [light or empty] occurs at a nominal location. Interchanging the stainless steel and low carbon steel laminations between top and bottom halves (second figure) creates an a_1 which can be used to compensate the measured a_1 in a magnet. Increasing the number of low carbon steel magnetic laminations increases the integral transfer function (third figure). An adjustment (decrease) in both a_1 and integral transfer function can be obtained together by mixing the two schemes in the same magnet (bottom figure).

5.3.1. Yoke Length for Integral a_1 Correction

Among the non-allowed measured harmonics, a_1 (skew quadrupole) had a magnitude large enough to be of concern in SSC dipoles. The major source of geometric a_1 in the dipole magnets is an up-down asymmetry in the coil. This a_1 is primarily related to variations in the components and the manufacturing process of the coils resulting in a difference between the top and bottom. This top-bottom difference is generally of a random nature and is the major source of the random variations in the geometric a_1 in the superconducting dipoles. A good correlation is expected for the measured a_1 in the collared coils before and after they are placed in the yoke.

In this section a method is presented that compensates for the measured a_1 in the collared coil by deliberately introducing another asymmetry in the yoke magnetic length between the upper and lower halves of the magnet. The method is schematically shown in Fig. 5.3.1. This correction would be adopted near the ends of the two coils in the magnet. The location where this correction would be implemented is the place where a change from the low carbon steel laminations to the stainless steel laminations takes place in the magnet end. A difference in the magnetic length between the top and bottom yoke halves is generated by switching the two types of laminations between the upper and lower halves. In order to adopt this scheme, one would first measure the a_1 in the collared coil at room temperature. This would determine the total number of laminations needed to be switched between the top and bottom halves of the magnet.

It is estimated that to correct 1 unit of a_1 in the SSC dipole one would need to switch ~ 25 mm of magnetic laminations with the same length of stainless steel laminations. The total amount of either type of the laminations used in the magnet would not change in the process. To first order, it would not change the allowed harmonics. In the 2-d cross-section of the magnet, it locally creates ~ 200 units of a_1 when normalized to the local field. The actual contribution is somewhat smaller since the field in this transition region is $\sim 85\%$ of the field in the straight section of the magnet. The actual 3-d end calculations give slightly different numbers and show a change in the a_1 correction [126] at high fields due to iron saturation. Other harmonics introduced in the process are a_3 , a_5 , etc. However, they all are $\sim .01$ unit or less, which is well within their specifications.

This a_1 correction scheme should be relatively simple to implement, particularly in the BNL-type horizontally split yoke designs where the geometry of the non-magnetic stainless steel and magnetic low carbon steel lamination is identical. It may, for example, be implemented in the following manner:

- The usual thickness of a pack of laminations in the body of BNL-built SSC prototype magnets is 76.2 mm. This pack could be made of 6.35 mm thick laminations. The same thickness and cross section should be used in both the magnetic and the stainless steel laminations.
- The amount of the two types of laminations used in any magnet is always the same and it is independent of the amount of the a_1 correction to be applied. Only the location of their placement in the magnet changes.
- A mis-match of a single 6.35 mm thick lamination in one end corrects $\sim \frac{1}{8}$ unit of a_1 . The actual switch between top and bottom creates twice the length of a mis-match. Therefore each switch of a lamination corrects $\sim \frac{1}{4}$ unit of a_1 .
- Make the magnetic measurement in the collared coils before they are put in a iron yoke. Decide how the two types of laminations should be distributed between the top and bottom halves of the magnet based on the measured a_1 in the collared coil. Note that if the measured a_1 is zero then the change over from magnetic to non-magnetic laminations would occur at the same axial location in the top and bottom halves of the magnet.

In the BNL-built SSC 50 mm dipole design, the length of the coil straight section is 14.859 meter and the length of the space occupied by low carbon steel laminations is 14.783 meter. The length of the space occupied by the stainless steel laminations is 150 mm in each end. With this geometry one can easily correct a few units of a_1 before getting into a region where the correction becomes highly non-linear or may significantly change the peak field distribution on the conductor. This change should give an adequate correction based on the expected maximum a_1 in most magnets or based on the measured a_1 in the prototype magnets.

5.3.2. Yoke Length for Integral Transfer Function Correction

The measured integral transfer function in the magnets may be different from the value expected from calculations. The difference in measured integral field could also be observed between two series of magnets built on the same design but by two manufacturers with two different sets of toolings. This was observed in HERA magnets [113,179]. This difference is of concern when these magnets are connected in series over the same power supply.

As mentioned earlier, the laminations used in the ends of the SSC magnets are made of non-magnetic stainless steel and the laminations used in the body (straight section) are made of magnetic low carbon steel. The place of transition from the magnetic steel to the non-magnetic steel laminations is somewhat flexible. An adjustment in the length (amount) of magnetic laminations to the stainless steel laminations for a fixed total mechanical length (amount), can be used as a parameter to adjust integral transfer function (see Fig. 5.3.1). This adjustment could either be applied to obtain a systematic change in the value to accommodate a systematic difference in transfer function between two manufacturers or to correct for a continuous upward or downward trend in transfer function during production. It could even be applied on a magnet by magnet basis after measurements (perhaps on the collared coil) to reduce the random variation in transfer function. Moreover, the proposed adjustment can be applied after the magnet tooling is made, a few magnets are constructed and magnetic measurements are performed. To reduce the random variation in transfer function, it may be adequate to measure the integral transfer function in the collared coil. The above adjustment then can be applied during the yoke assembly.

The feasibility of this scheme is examined here. The measured systematic difference in the transfer function between the two series of HERA dipole magnets [113,179] manufactured by two vendors was $\sim 2 \times 10^{-3}$. The required adjustment to correct the above difference in SSC magnets is evaluated here. In SSC dipole magnets, the yoke contributes $\sim 25\%$ to the transfer function at injection and $\sim 22\%$ at the maximum design field. The design magnetic length of the dipole was 15 meter. Therefore to adjust 2×10^{-3} at injection one would change the material of yoke laminations in a length by ~ 12 cm. To implement such a scheme in practice, one would start with a magnet design in which the total magnetic lamination length is reduced (or conversely the total stainless steel lamination length is increased) from a typical value. To contain the leakage (fringe) field in that region, if required, one could have low carbon steel laminations with an increased inner diameter. The stainless steel laminations then could be put in-between the collar and the increased

yoke inner diameter. The later would decrease the efficiency of the proposed scheme only by a small amount as compared to the case when all end laminations were made of stainless steel only.

Methods to adjust a current dependence in the skew quadrupole harmonic (a_1) in dipoles have been discussed earlier. To adjust a current dependence in transfer function, one could adjust the packing factor of magnetic, low carbon steel laminations in the body (straight section) of a magnet. This adjustment in the current dependence has been applied in the 80 mm aperture RHIC arc dipoles.

5.4. Conclusions on the Field Quality Improvements after Construction

The methods described in this chapter show that it is possible to build superconducting magnets having relative field errors ($\frac{\Delta B}{B}$) only a few parts in 10^{-5} instead of the usual errors of a few parts in 10^{-4} at $2/3$ of the coil radius. This improvement in field quality is crucial to the high luminosity performance of RHIC and could be important to all high energy colliders.

The tuning shim method described overcomes the limitations in field quality posed by manufacturing tolerances. It compensates for the field errors in the body of the magnet. The second proposed method makes a lumped correction at the magnet ends. Though this has been proposed here for compensating integral a_1 , it can be used for compensating other harmonics also.

Eight tuning shims are used to independently correct eight measured harmonics in the 130 mm aperture RHIC insertion quadrupoles. The tuning shims are installed after the cold-mass has been assembled. This does not require opening the magnet, which not only makes the process more efficient but also more reliable. If a magnet is opened and assembled again, there may be a slight change in field harmonics which can not be neglected in these high field-quality magnets.

Good agreement has been found between the calculations and measurements based on the data available so far. A series of warm measurements have been performed to make comparison over a wide range of tuning shims. These results show that the effects can be reliably computed at low fields. Magnetic measurements at the design current (5 kA) were also performed to complete a comparison between the calculations and measurements. The algorithm to compute the tuning shim thickness is based on these measured changes in harmonics at 5 kA.

The method of tuning shims (or a simplified version of it) can also be adopted in a large scale magnet production program. In that case the number of tuning shims can be reduced to correct only a few important harmonics. This could relieve the tolerances on parts, assembly and general manufacturing process while assuring a good field quality in a plan suitably adopted for the industrial magnet production environment.